LA-UR- 94-3445

Conf-9408181--1

Los Alamos National Laboratory is operated by the University of California for the United States Department of Energy under contract W-7405-ENG-36

TITLE: THEORY OF HF INDUCED TURBULENCE IN THE IONOSPHERE: STATUS AND CHALLENGES

AUTHOR(S): D.F. DuBois, T-13

SUBMITTED TO: Presented at the IVth Suzdal URSI Symposium on Artificial Modification of the Ionosphere, Uppsala, Sweden, August 14-20, 1994

Los Alamos

Los Alamos National Laboratory
Los Alamos, New Mexico 87545

FORM NO. 836 R4
ST. NO. 2629 5/81

Theory of HF Induced Turbulence in the Ionosphere: Status and Challenges[1]

D. F. DuBois[2]
Los Alamos National Laboratory, MS B213
Los Alamos, NM 87545 USA

Abstract

In the past five years the combination of new theoretical concepts and computer simulations along with dramatically improved observational diagnostics appear to have led to a detailed, quantitative, understanding of the properties of the Langmuir turbulence induced in the unpreconditioned ionosphere at Arecibo during the first tens of milliseconds following the turn-on of the HF heater. This is the only observational regime in which the initial ionospheric conditions are known to a high level of confidence. The so called strong Langmuir turbulence (SLT) theory predicts observed features in this early time heating which are completely at odds with the prediction of the traditional weak turbulence approximation. The understanding of the observed signatures for times greater than say 30-50 ms following the onset of heating at Arecibo is still incomplete. The same is apparently true for the observations at Tromsø where the unique predictions of SLT theory are not so clearly observed. Density irregularities, induced by heating at Arecibo and perhaps present in the ambient ionosphere at Tromsø, appear to control the properties of the turbulence. The proper description of the coexistence of Langmuir turbulence with various density irregularities and accounting for the turbulent modification of the electron velocity distribution are challenges for the theory.

In this paper I will review, starting from the Vlasov-Poisson equations, the fundamental basis of the reduced models used to describe SLT and suggest improvements to the standard model including a new local quasi linear theory for the treatment of hot electron acceleration and transit time damping or burnout of collapsing Langmuir cavitons.

The increased ponderomotive and thermal pressures of the horizontal, Airy layered, turbulence observed by Djuth et.al. are predicted to be large enough to induce density depletions of a few percent which in turn can alter the standing wave profile of the heater. These turbulence-induced pressures, which are strong functions of the local heater intensity, are expected to lead to an enhanced filamentation instability of the heater field near reflection density which can evolve into intermediate scale field aligned density irregularities.

New SLT simulation diagnostics reveal that the Langmuir waves and ion acoustic waves participating in the decay-cascade processes, near or below matching density, are confined to field aligned density depletion channels or filaments. This leads to the speculation that these may be the seeds for short scale striations which are observed to be correlated with the Langmuir turbulence.

---

[1] Review Paper presented at the IVth Suzdal URSI Symposium on Artificial Modification of the Ionosphere, Uppsala, Sweden, August 14-20, 1994.

[2] Research carried out in collaboration with Harvey A. Rose and David Russell.

1. Introduction

Twenty three years ago, Perkins and Kaw [1971] predicted that absorptive parametric instabilities [DuBois and Goldman, 1965] could be excited in the F layer of the ionosphere by powerful radio (HF) transmitters. Soon thereafter, Carlson et.al. [1972] and Wong and Taylor [1971] observed HF enhanced plasma lines using the Arecibo incoherent scatter radar. Two decades of intense observational and theoretical work followed. The 1980's saw the development of new theoretical models and improved observational diagnostics.

In this review I will concentrate on observations, mainly carried out at Arecibo over the last five years, which have attained unprecedented temporal and spatial resolution of the HF induced Langmuir turbulence as observed by the incoherent scatter radar. This work was motivated by new predictions of the so called strong Langmuir turbulence (SLT) theory and the observations, in turn, contributed to the further development of the theory. This theory predicted properties of the turbulence induced near reflection density which appeared to be in substantial agreement with the observations and which were totally different than the predictions of the traditional weak turbulence approximation (WTA).

Despite this apparent success of SLT theory a number of workers expressed doubts concerning the value of this theory. Stubbe et.al. [1992] expressed doubts concerning the fundamental correctness of the model and alleged that its predictions did not agree with observations at Tromsø. However, Kohl et.al. [1994] have recently reported VHF radar observations at Tromsø which may have identified the SLT-predicted continuum plus free-mode plasma line features as well as the $\omega = 0$ ion line feature. [See also Kohl et.al. 1993, especially Fig. 10]. Also Isham et.al. [1994], using their chirped radar technique, observed up-shifted plasma line features in the UHF radar spectrum near reflection altitude at Tromsø; the upshift is consistent with a free-mode line. Muldrew [1994, Comment] alleged that SLT theory could not explain certain longer time heating phenomena at Arecibo and promoted a field aligned duct hypothesis which he claimed could explain essentially all the observations. It should be emphasized that no other quantitative, nonlinear calculations on the same level as the SLT predictions have been made using alternative theories. Several allegations stated that SLT theory could not explain certain observational regimes where, in fact, no SLT predictions had been attempted because of technical difficulties.

In this review I will summarize some of the recent apparent successes of SLT theory but I will concentrate on the problems remaining in formulating accurate models and in calculating the predictions of these models for ionospheric conditions which are relevant to the observations.

In Section 2, I will summarize recent work [DuBois et.al. 1994b] in which we have attempted to derive improved, but numerically tractable, reduced SLT models starting from kinetic theory. Validity conditions specifying an extended "Zakharov" ordering are given. This has resulted in a more accurate description of the low frequency ion response for the case of nearly equal electron and ion temperatures appropriate to the ionosphere. The predictions of spectral simulations using the improved model are qualitatively similar to those of the older generalized Zakharov model. We have also introduced a new local quasilinear theory which gives a kinetic description, on the slow time scale (compared to the HF period), of the collisionless damping of cavitons and the concomitant evolution of the electron velocity distribution.

In Section 3, I review the predictions of SLT models for a smooth, unpreconditioned ionosphere. These are in apparent quantitative agreement with the recent height and time resolved observations of Sulzer and Fejer [1994] for the first tens of milliseconds of heating from a quiet start. At later times discrepancies appear such as the observations of isolated free modes and decay-cascade spectra from altitudes above the unperturbed matching altitude. There appears to be agreement that some of these discrepancies might be explained if density irregularities develop on the time scale of tens of ms following a quiet start. The unique predictions of SLT theory are not so clearly or regularly observed at Tromsø [Djuth et.al. 1994]. This may be the result of the existence of density irregularities at Tromsø which are in the ambient ionosphere or which grow much more rapidly than at Arecibo.

This leads in Section 4 to speculations on how self-consistent theories might be constructed of Langmuir turbulence in coexistence with density irregularities. Among these are horizontal density depletions about 50 meters thick which occur at the interference maxima of the heater and are caused by the ponderomotive (and thermal) pressures of the induced Langmuir turbulence. Self-focusing of the heater results in km scale irregularities. It is argued that again the thermal and ponderomotive pressures of the Langmuir turbulence electric fields greatly dominate those of the heater itself and a proper theory of heater filamentation must, therefore, take into account the induced turbulence.

In Section 5, I present preliminary evidence and theoretical arguments that at densities in the decay-cascade regime SLT theory predicts Langmuir filaments which may be the seeds for short-scale field-aligned irregularities. These are density irregularities with transverse scales of say, 1 to 10 meters and longitudinal scales (along the geomagnetic field) several times larger. These sausage structures (relative to the geomagnetic field $\mathbf{B}_0$) analogous to the pancake caviton structures predicted near reflection density. The Langmuir waves participating in the decay-cascade spectra are apparently trapped in these sausages and diffraction effects broaden the LW spectrum, to contain $\mathbf{k}$ vectors making large angles with $\mathbf{B}_0$. Thus these filaments which are an intrinsic, self-consistent, prediction of SLT partially fulfill the role which Muldrew [1978-1994] ascribes to his postulated field aligned ducts. The Langmuir filaments are apparently the nonlinear saturated state of the transverse modulational instability of the point decay-cascade spectrum which was approximately studied by Rubenchik and Shapiro [1991, 1992]. In three dimensions these filaments are predicted to collapse to small transverse dimensions where they are burned out by Landau damping.

2. Kinetic Theory Basis of SLT Models

There have been many derivations, usually starting from fluid equations, of the generalized Zakharov models used in SLT studies, e.g. [Zakharov 1972, Nicholson 1983]; Formal derivations starting from kinetic theory have been made by Stubbe [1990] and Goodman [1992]. Here I will summarize the results of a recent paper [DuBois, Russell and Rose, 1994b] which I will refer to as I. In this paper we have tried to formulate improved SLT models which are computationally tractable. The kinetic issues are well-known: 1. The ionospheric plasma has nearly equal electron (T_e) and ion (T_i) temperatures, which results in strongly damped ion acoustic waves (IAWs) which are poorly described by the fluid equations. 2. Collisionless damping of Langmuir waves (LWs) which is also important for the burnout of collapsing Langmuir cavitons, must be added in an ad hoc way to the fluid equations and depends sensitively on the electron velocity distribution. 3. The standard model is isothermal and does not allow for the temporal evolution of the electron and ion distribution functions.

The starting point is the Vlasov equations for evolution of the electron ($\sigma = e$) and ion

$(\sigma = i)$ distribution functions:

$$\{\partial_t + \mathbf{u} \cdot \nabla + q_\sigma/m_\sigma(\mathcal{E} + \mathbf{u} \times \mathbf{B} \circ c^{-1}) \cdot \partial_u\} f^\sigma(\mathbf{u}, \mathbf{x}, t) = 0 \tag{1}$$

where the total electric field $\mathcal{E}$ is determined (apart from a spatially uniform heater field) by Poisson's equation (in Gaussian units)

$$\nabla \cdot \mathcal{E} = \sum_\sigma 4\pi e q_\sigma \int d^D u f^\sigma \tag{2}$$

Here D is the dimensionality of space.

We account for the effect of a uniform background geomagnetic field, $\mathbf{B}_0$. consider $\mathcal{E}$ to have a high frequency component $\mathbf{E}_H$ (mainly at a frequency near the heater frequency ω_{HF}) and a low frequency longitudinal component $\mathbf{E}_L : \mathcal{E} = \mathbf{E}_H + \mathbf{E}_L$. It is convenient [see Bezzerides et.al. 1976] to transform away the cold plasma motion where the particle jitter velocities satisfy

$$m_\sigma \dot{\mathbf{u}}_{H\sigma} = q_\sigma(\mathbf{E}_H + \mathbf{u}_{H\sigma} \times \mathbf{B}_0 c^{-1}) \tag{3}$$

The low frequency longitudinal field can be written as a gradient of a low frequency potential $\phi_L : \mathbf{E}_L = -\nabla\phi_L$.

We can define the distribution functions $F^\sigma(\mathbf{v}, \mathbf{x}, t)$ in the local oscillating frame by

$$F^\sigma(\mathbf{v}, \mathbf{x}, t) = f^\sigma(\mathbf{u}_{H\sigma} + \mathbf{v}, \mathbf{x}, t) \tag{4}$$

which is easily seen to obey [Bezzerides et.al. 1977]

$$\{\partial_t + \mathbf{v} \cdot \nabla + [q_\sigma/m_\sigma)(\mathbf{E}_L + \mathbf{v} \times \mathbf{B}_0 c^{-1}) - m_\sigma^{-1}\mathbf{P}^\sigma] \cdot \partial_v\} F^\sigma \tag{5}$$

$$= \left[\mathbf{u}_{H\sigma} \cdot \mathbf{v}, F^\sigma\right]$$

where on the right hand side occurs the Poisson bracket defined by

$$\left[A, B\right] \equiv \nabla A \cdot \partial_v B - \partial_v A \cdot \nabla B \tag{6}$$

Here P^σ is a force (related below to the ponderomotive force) defined as

$$m_\sigma^{-1}\mathbf{P}^\sigma = (\mathbf{u}_{H\sigma} \cdot \nabla)\mathbf{u}_{H\sigma} \tag{7}$$

This oscillation center formulation is convenient because it provides a clean separation of cold fluid effects and thermal and kinetic effects. The current of species σ is just

$$\mathbf{J}^\sigma = q_\sigma \mathbf{u}_H^\sigma n^\sigma + q_\sigma \int d^D v \mathbf{v} F^\sigma \tag{8}$$

where $n^\sigma = \int d^D v F^\sigma$. The first term is just the cold fluid current while the second term contains thermal dispersion and collisionless damping effects. Ponderomotive effects are also immediately accounted for in (5) – (they arise in cold fluid theory) – since the time average of $\mathbf{P}^\sigma$ over a heater cycle, which we call $\mathbf{P}_0^\sigma$, is just the ponderomotive force which is complicated if the full dependence of $\mathbf{u}_{H\sigma}$ on the magnetic field $\mathbf{B}_0$ (determined from (3)) is retained.

However, these $\mathbf{B_0}$ corrections are of order $(|\mathbf{E}|^2/4\pi n_0 T_e)(\Omega_e^2/\omega_p^2)$, where $\Omega_e = eB_0/mc$ is the electron gyro frequency, and are consistently negligible in the extended Zakharov ordering discussed below. Then $\mathbf{P}_0^\sigma$ becomes the familiar ponderomotive force

$$\mathbf{P}_0^\sigma = \nabla\phi_p^\sigma; \quad \phi_p^\sigma = \frac{q_\sigma^2|\mathbf{E}_1|^2}{4m_\sigma}\omega_p^2 \tag{9}$$

where ϕ_p^σ is the ponderomotive potential and $\mathbf{E}_1$, is the envelope field of $\mathbf{E}_H$:

$$\mathbf{E}_H = \frac{1}{2}\mathbf{E}_1 e^{-i\omega_p t} + c\cdot c. \tag{10}$$

Because of the mass dependence of $\mathbf{u}_{Hi}(\alpha m_i^{-1})$ both the ponderomotive force and the Poisson bracket term can be neglected for ions. The ions respond to the low frequency electric field and $\mathbf{B_0}$.

The difference $\mathbf{P}^\sigma - \mathbf{P}_0^\sigma$ is essentially at frequency $2\omega_{HF} \sim 2\omega_p$ where the plasma can respond only weakly. If this is neglected the left hand side of (5) has no explicit high frequency dependence while the Poisson bracket operator on the right has explicit high frequency dependence which couples the high frequency part of F^σ to its low frequency part. It is convenient then to separate F^σ into high and low frequency parts

$$F^\sigma = F_0^\sigma + F_1^\sigma e^{-i\omega_p t} + F_{-1}^\sigma e^{i\omega_p t}. \tag{11}$$

When $\mathbf{u}_H^\sigma$ can be considered small, in a sense defined below, we can iterate to get a set of equations connecting F_0^σ and $F_{\pm 1}^\sigma$. A more complete treatment accounting for frequency components at higher harmonics of ω_p is found in I.

For the low frequency behavior we obtain a Local Quasilinear Equation (see I for details)

$$\{\partial_t + \mathbf{v}\cdot\nabla + (e/m)(\nabla\phi_L + \nabla\phi_p^e - \mathbf{v}\times\mathbf{B}_0 c^{-1})\cdot\partial_v\}F_0^e(\mathbf{v},\mathbf{x},t)$$

$$= \frac{e^2}{m^2\omega_p^2} Re\int dx'_{\|}[\mathbf{v}\cdot\mathbf{E}_1(\mathbf{x},t), g(v, x_{\|} - x'_{\|})] \tag{12}$$

$$\times[\mathbf{v}\cdot\mathbf{E}_1^*(\mathbf{x}',t), F_0^e(\mathbf{v},\mathbf{x}',t)]$$

where Re signifies real part and the free electron propagator is

$$g(v, x_{\|} - x'_{\|}) = \frac{1}{v}\ exp\ [i\frac{\omega_p}{v}(x_{\|} - x'_{\|})]H(\frac{x_{\|} - x'_{\|}}{v}) \tag{13}$$

Here $x_{\|}$ is a coordinate in the direction of v and $\mathbf{x}_\perp$ is the coordinate vector in the orthogonal direction and H() is the Heavyside or step function. The right hand side is written only for the case where the straight line orbit approximation is valid for the propagator which requires $1/2\ mv^2 >> max(e\phi_L, e\phi_p^e)$. This is usually the case for resonant particles since the shortest spatial scales observed in SLT simulations, i.e. during collapse, have k about 0.1 k_D implying resonant velocities $\sim$ 10 ve. For ionospheric applications we should take into account the effect of the geomagnetic field, $\mathbf{B_0}$, on the unperturbed cyclotion orbits by in the propagator (13) (see also I). On the average if the electron Larmor radius, v/Ω_e, is greater than the correlation length of the turbulent E fields, ℓ_c, then the deviation from straight line orbits

can be ignored. This leads to the condition $v/v_e >> (\ell_c/\lambda_p)(\Omega_e/\omega_p)$. In the cavitation regime the right hand side of this inequality is of order unity, implying that the use of straight line orbits is justified for superthermal electrons.

In general the iterative procedure used to obtain (10) and other results below requires the extended Zakharov ordering:

$$\epsilon_0 = \frac{|\mathbf{E}_1(\mathbf{x},t)|^2}{4\pi n_0 T_e} \ll 1, \frac{n(\mathbf{x},t)}{n_0} \ll 1, (k\lambda_{De})^2 \ll 1, \omega/\omega_{pe} \ll 1, \frac{\Omega_e^2}{\omega_{p_e^2}} \ll 1$$

$$\frac{\delta v_e^2(\mathbf{x},t)}{< v_e^2 >} \ll 1 \quad \text{and} \quad \epsilon_0^2 \ll \frac{v^2}{< v_e^2 >} \ll \epsilon_0^{-2}. \tag{14}$$

We consider these small quantities to be of the same order. The last two listed are kinetic conditions. Here $\delta v_e^2(\mathbf{x},t) \simeq \int d^D v v^2 \delta F_0^e / < n >$ is a measure of the local fluctuation in the electron temperature and $\langle v_e^2(t) \rangle$ the spatial average. It is easy to see that (12) conserves electron number. It can also be shown that for a homogeneous plasma the spatial averaged distribution, $\langle F_0(\mathbf{v},t) \rangle$, obeys the standard quasilinear evolution equation where the diffusion operator depends on the Langmuir spectrum $\langle |E_1(\mathbf{k})|^2 \rangle$ evaluated at $k_{||} = \omega_p/v$.

For ions the ponderomotive force and the quasilinear "collision" term involving the high frequency fields can be neglected to terms of order m_e/m_i:

$$\{\partial_t + \mathbf{v} \cdot \bigtriangledown - (Ze/m)(\bigtriangledown \phi_L - \mathbf{v} \times \mathbf{B}_0 c^{-1}) \cdot \partial_v\} F_0^i(\mathbf{v},\mathbf{x},t) = 0. \tag{15}$$

The ions effectively see only the low frequency longitudinal potential ϕ_L which obeys

$$\bigtriangledown^2 \phi_L = -4\pi \sum_\sigma q_\sigma \int d^D v F_0^\sigma(\mathbf{v},\mathbf{x},t). \tag{16}$$

Quasilinear diffusion of electrons and ions caused by fluctuations in the **low** frequency potential field can be treated by standard methods (see I) and will not be discussed here.

We have reduced the full kinetic theory problem to an approximate one, valid in the extended Zakharov ordering, which involves only the slowly varying parts, F_0^e and F_0^i, of the distribution functions. These evolve on the same slow time scale as the usual Zakharov equation variables; the electric field envelope and the density perturbation.

For low velocity electrons, in the main body of the distribution function, the right hand side of (10) can be dropped. If we consider a small non uniform perturbation $\delta F_0^\sigma e^{i(\mathbf{k}\cdot\mathbf{x}-\omega t)}$ superimposed on the spatial averaged distributions $\langle F_0^\sigma(v) \rangle$ and apply standard linear stability techniques to (12) and the corresponding equation for F_0^i we find that the low frequency electron density perturbation $n_e(\mathbf{k},\omega)$ satisfies

$$D(\mathbf{k},\omega) n_e(\mathbf{k},\omega) \equiv \left[\frac{\epsilon_L(\mathbf{k},\omega)}{(1+\chi_i(\mathbf{k},\omega))\chi_e(\mathbf{k},\omega)}\right] n_e(\mathbf{k},\omega) = \frac{k^2}{4\pi e} \phi_p^2(\mathbf{k},\omega) \tag{17}$$

where χ_e and χ_i are the standard collisionless susceptibilities of electrons and ions (including a uniform magnetic field B_0) and $\epsilon_L = 1 + \chi_e + \chi_i$ is the longitudinal dielectric function. Equation (17) is the appropriate generalization of the second Zakharov equation which takes

into account the exact, linear, low frequency density response. The linearization employed here can be shown to be valid if $n_e/n_o \ll 1$ and $|u_H^e|^2/v_e^2 \ll 1$ which imply that electron or ion trapping in the low frequency waves is negligible.

Equation (17) as it stands, as well as other formal kinetic approaches [e.g. Stubbe 1990], are not useful for turbulence simulations since when transformed back to the time domain they result in operators that are nonlocal in time. The electron susceptibility is no problem since $\omega \ll kv_e$ for the low frequency waves where $\chi_e(\mathbf{k},\omega) = k_{D_e}^2/k^2 + i\sqrt{\frac{\pi}{2}}\frac{\omega}{kv_e}e^{-\frac{\omega^2}{2k^2v_e^2}}$. The ion susceptibility is the problem since $\omega \sim kv_i$ for ion acoustic waves when $T_e \simeq T_i$ and simple asymptotic limits do not apply. The problem is to get a simple but accurate approximation to the operator $D(\mathbf{k},\omega)$ defined in (17). We have used a simple 3-pole Padé approximant for $\chi_i(\mathbf{k},\omega)$ that produces the exact value of $D(\mathbf{k},\omega)$ at $\omega = 0$ and therefore reproduces the exact modulation instability (or OTSI) threshold and growth rate, reproduces exactly the parametric decay instability (PDI) threshold and growth rate and has the correct asymptotic limit as $\omega \to \infty$. This approximant is a variant of the 3 pole approximation of Hammett and Perkins [1991]. Goldman, Newman and Perkins [1993] have introduced a four pole approximant; this has not been applied to the problems which we address here. Our result, which has been previously published [DuBois et.al. 1993], is a generalized second Zakharov equation for the time evolution of $n_e(\mathbf{k},t)$:

$$[\partial_t + \sqrt{2}\, kv_i y_0(R)]\{\partial_t^2 + 2\nu_{0i}kc_s\partial_t + k^2c_s^2\}n_e(\mathbf{k},t)$$

$$= -\frac{k^2}{16\pi m_i}[\partial_t + \sqrt{2}\, kv_i y_0(\infty)]|\mathbf{E}_0(t) + \mathbf{E}|_{\mathbf{k}}^2. \tag{18}$$

Here $R = 1 + T_e/T_i, v_i$ is the ion thermal speed, and $y_0(R)$ is the purely complex root of $D(\mathbf{k},\omega)$ in the 3 pole approximation. The ion acoustic speed c_s and the ion acoustic damping coefficient are determined from the two real roots. The dependence of these roots on T_e/T_i is given in I. As T_e/T_i becomes large $y_0(R) \to y_0(\infty)$ and the operators in square brackets on each side of (18) tend to cancel and (18) "heals" back to the standard second Zakharov equation involving only the operator in curved braces. There is no need to transform (18) back to real space since we will numerically solve it using spectral methods. In obtaining the ponderomotive term in (18) we have written $\mathbf{E}_1 = \mathbf{E}_0(t) + \mathbf{E}$, where $\mathbf{E}_0(t)$ represents the uniform HF heater field:

$$\mathbf{E}_0(t) = \mathbf{E}_0 \;\; exp \;\; (-i\Delta\Omega t) \;\; ; \Delta\Omega = \omega_{HF} - \omega_p \tag{19}$$

where $\Delta\Omega/\omega_p \ll 1$.

By $|\mathbf{E}_0(t) + \mathbf{E}|_{\mathbf{k}}^2$ we mean the $\mathbf{k}$ Fourier component of the absolute square of the fields. Predictions, using this modified equation, for the spectra observed in HF heating are given in I and in Section 3 of the present paper.

Equation (18), which models the intrinsic nonlocality in time by involving higher time derivatives, is easily integrated to study the temporal evolution of the turbulence. In I we also study the dependence of the operator $D(\mathbf{k},\omega)$ on the external magnetic field. Except for angles of $\mathbf{k}$ within the range $\Delta\theta \sim (m_e/m_i)^{1/2} \sim 10^{-2}$ of perpendicularity to $\mathbf{B}_0$ the values of $D(\mathbf{k},\omega)$ for $B_0 = 0$ (including the 3 pole approximant) are a good approximation to the magnetized case. [The value of $D(\mathbf{k},\omega = 0)$ is exactly the same in the magnetized and unmagnetized case for all $\mathbf{k}$.]

Another approach to the ion dynamics problem has been recently presented by Helmersen and Mjølhus [1994]. Working in one spatial dimension they replaced the usual low frequency Zakharov equation by the linearized ion Vlasov equation. They also found good qualitative agreement with the predictions of the usual Zakharov models. Their approach should be more accurate than our 3 pole approximation to the ion dynamics. The two approaches have not, however, been compared in detail.

The equation for the envelope $\mathbf{E}_1$ of the high frequency field $\mathbf{E}_H$ is obtained from the second time derivative of Poisson's equation

$$\nabla \cdot \frac{\partial^2}{\partial t^2}\mathbf{E}_H = -4\pi \nabla \cdot \frac{\partial}{\partial t}\mathbf{J}_H^e \tag{20}$$

or introducing the envelope field $\mathbf{E}_1$ from (10) and an analagous envelope representation for $\mathbf{J}_H$ we have

$$\nabla \cdot [2i\omega_p \partial_t \mathbf{E}_1 - \omega_p^2 \mathbf{E}_1] \simeq 4\pi i \omega_p \nabla \cdot \mathbf{J}_1^e \tag{21}$$

assuming that the envelopes evolve on the slow time scale i.e. $|\partial_t \mathbf{E}_1| \ll \omega_p |\mathbf{E}_1|$ and $|\partial_t \mathbf{J}_1^e| \ll \omega_p |\mathbf{J}_1^e|$. From (8) (3) (10) and (11) we have

$$\mathbf{J}_1^e = \frac{e^2 n_0}{im\omega_p}\mathbf{E}_1 - e\int d^D v \mathbf{v} F_1^e(x,v,t) \tag{22}$$

We can relate F_1^e to F_0^e using (5) and (11).

The resulting equation for $\mathbf{E} = \mathbf{E}_1 - \mathbf{E}_0(t)$ is found to be

$$\nabla \cdot \left[i2\omega_p(\partial_t + \nu_{ec} + \nu_e \bullet) + 3 < v_e^2 > \nabla^2 - \Omega_e^2 \frac{\nabla_\perp^2}{\nabla^2} - \omega_p^2 \frac{n}{n_0} \right] \mathbf{E} \tag{23}$$

$$= \mathbf{E}_0(t) \cdot \frac{\nabla n}{n_0}\omega_p^2$$

where $< v_e^2 > \equiv 2m_e T_e \equiv \int d^D v v^2 < F_e^0(v,t) >$. We have written the damping as the sum of a collisional damping $\nu_{ec} = \frac{1}{2}\nu_{ei}$, where ν_{ei} is the electron-ion collision frequency and a collisionless damping.

In the Local Quasilinear Theory the collisionless damping operator is defined by

$$\nu_e \bullet \mathbf{E} \equiv \frac{\omega_p}{2n_0}\int d^D v \int dx_\parallel' e^{i\omega_p(x_\parallel - x_\parallel')/v} [\mathbf{v} \cdot \mathbf{E}(x_\parallel', \mathbf{x}_\perp, t), F_0^e(\mathbf{v}, x_\parallel', \mathbf{x}_\perp, t)] \tag{24}$$

The definition of the Poisson bracket is given in (6) and $x_\parallel, \mathbf{x}_\perp$ are defined as for (12). This damping depends, in general, on the spatial modulation of the slowly varying part of the electron distribution function. If we write $F_0^e =< F_0^e > + \delta F_0^e(\mathbf{v}, \mathbf{x}, t)$ and neglect the spatially dependent fluctuation δF_0^e then it can be shown that the damping operator reduces to

$$\nu_e \bullet \mathbf{E} = \int d^D x \nu_e(\mathbf{x} - \mathbf{x}')\mathbf{E}(\mathbf{x}', t) \tag{25a}$$

where

$$\nu_e(\mathbf{k}) = \int d^3(\mathbf{x} - \mathbf{x}') e^{-i\mathbf{k}\cdot(\mathbf{x}-\mathbf{x}')} \nu_e(\mathbf{x} - \mathbf{x}') \tag{25b}$$

$$= \frac{\pi\omega_p^3}{k^2 n_0} \int d^D v \delta(\omega_p - \mathbf{k}\cdot\mathbf{v})\mathbf{k}\cdot\partial_{\mathbf{v}}\langle F_0^e(\mathbf{v},t)\rangle$$

which is the usual Landau damping often used in SLT models. This damping as well as the thermal dispersion, $3k^2 < v_e^2 >$, of Langmuir waves, evolve in time as the distribution $< F_0(\mathbf{v},t) >$ evolves. The proper accounting for this evolution of the background distribution function can be important for HF induced turbulence for longer times after the onset of heating from a cold start or in preconditioned cases. Bulk heating which increases $< v_e^2 >$ will tend to weaken the turbulence by decreasing $< |E_0|^2 > /4\pi n T_e$ which is the strength parameter [Gavrilov et.al. 1994, Wang et.al. 1993]. The effect of $\mathbf{B}_0$ on the Landau damping is discussed in I.

The neglect of the spatial fluctuation in $F_0^e(\mathbf{v},\mathbf{x},t)$, which leads to the usual Landau damping operator, may not be a good approximation. In Fig. 1 we show the results of a ID Vlasov simulation carried out by J.G. Wang [1993, 1994] for a case with initially $T_e = T_i$ and $E_0^2/16\pi n_0 T_e = 3.125\times10^{-2}, \omega_0 = \omega_{p_e}$, and $m_i/m_e = 1836$. In the left hard panels of Fig. 1 we show the electric field envelope $|E(x,t)|^2$ and the ion density perturbation $\delta n_i/n_0$ at the time when the caviton's electric field reaches its maximum amplitude. In the right hard panels of Fig. 1 we show the electron and ion phase space contours at the same time. We see that there is a strong local distortion of the electron distribution at the caviton location with jets of accelerated electrons in both directions. Weaker jets further away from the caviton were emitted in the earlier development of the caviton at previous maxima of the electric field; i.e. jets are emitted every plasma period. The ion distribution is more mildly perturbed in the center of the caviton consistent with the ejection of density from the region. At a slightly later time jets of ejected ions are also seen. This is one example of many from these Vlasov simulations which lead me to believe that **local** distortions of the distribution function may be important for the burn out of cavitons. Of course these simulations only include the behavior of the few collapse events. In a system of many cavitons after a sufficiently long time the spatial averaged distribution $< F_0^e(v,t) >$ will develop fast electron tails which may be as important as the locally generated tails in determining the collisionless damping. The relative importance of local and averaged distributions will depend sensitively on the size of the turbulent region and whether or not hot electrons leave the region or recirculate due to collisions [Gurevich 1985] or ambipolar fields.

It is a challenge to try to solve the coupled set of equations (18), (23) and (24), and (12) which describe–all on the slow time scale–the evolution of the turbulent fields and the local distribution functions.

3. Predictions of SLT models for a unperturbed, smooth ionosphere and comparison with observations

Here I will attempt to summarize the status of our understanding of the theoretical predictions of the HF induced turbulence in a smooth ionosphere which is not preconditioned by earlier HF interactions. A more complete and detailed discussion is given in DuBois et.al.[1993]. There is good evidence [Djuth et.al. 1994b] that this is often a valid picture of the ambient ionosphere at Arecibo which appears to have density fluctuations $\delta n/n_0 < 10^{-3}$. This may not be true at Tromsø where there is reason to believe [Djuth et.al. 1993] that the ambient ionosphere often contains density irregularities with $\delta n/n \sim 10^{-2}$ which can be a significant perturbation on the Langmuir turbulence.

Fig. 2, borrowed from DuBois et.al. [1993], is a schematic representation of the distribution of Langmuir turbulence at various altitudes, z, in a linear density profile as represented

by the dashed line for the local plasma frequency $\omega_p(z)$. The abscissa in these figures is the frequency of the incoherent radar spectra: In Fig. 2, which plots the up shifted plasma line spectra, the zero of frequency is at $\omega_{radar} + \omega_{HF}$. Because the correlation length of the turbulence (< several meters) is much smaller than the density scale length of the unperturbed ionosphere (20-100 km) it can be shown than the observed radar spectra is an incoherent sum (or integral) of spectra over the range of densities (or altitudes) within the resolution range of the radar detection scheme.

The turbulence signatures appear to have two limiting regimes [Hanssen et. al. 1992, DuBois et.al. 1993]: A near reflection density ($\omega_p(z) \sim \omega_{HF}$) "cavitation" regime and a lower matching density ($\omega_p(z) \simeq \omega_{HF}(1 - 3/2k_r^2\lambda_D^2)$) "decay-cascade" regime.

The cavitation regime lies in the first few heater interference (or "Airy") maxima near reflection density. As shown in the modal energy spectrum inset in Fig. 2, the spatial Fourier spectrum of Langmuir wave (LW) density fluctuations, $k^2 < |\mathbf{E}(k)|^2 >$ is a broad featureless spectrum in this regime. In the upper panels of Fig. 3 we show contours of the spectra, $k^2 < |\mathbf{E}(\mathbf{k})|^2 >$, computed in 2D simulations in I using equations (18) and (23) where the background distribution functions F_0^e and F_0^i are taken to be fixed in time and their spatial fluctuations are neglected. It is worth repeating the fact that a given radar which measures electron density fluctuations only at fixed wave vector $\mathbf{k}_r$ ($\simeq 2\mathbf{k}_{radar}$ for backscatter) observes only a tiny part of the turbulent spectrum. The power spectrum of the fluctuations measured by the radar, $< |E(\mathbf{k}_r, \omega|^2 >$, is shown schematically in Fig. 2 near the first Airy maximum to consist of a broad "caviton" continuum, resulting from dynamics of collapsing cavitons, with frequencies mostly below $\omega_{HF} \sim \omega_p$ plus an up shifted "free mode" feature resulting from LWs emitted during the collapse process. The free mode feature lies on the Langmuir wave dispersion line shown in Fig. 2. Computed power spectra from 2D simulations are shown in Fig. 4.

Most of the near reflection density predictions appear to have been verified – at early heating times in an unpreconditioned ionosphere – in a series of experiments culminating in the beautiful diagnostics of Sulzer and Fejer [1994] who achieved a spatial resolution of 150 m and a temporal resolution of 1 ms in their measured spectra. Earlier observations of Djuth et.al. [1986], Cheung et.al. [1989], Cheung et.al. [1991], and Fejer et.al. [1992], have demonstrated, with increasing sophistication, the essential validity of the SLT predictions for the near reflection Langmuir turbulence during the first 30-60 ms of HF heating in an unpreconditioned ionosphere at night. The predictions of the older weak turbulence approximation are totally at odds with the observations.

Sulzer and Fejer [1994] have clearly observed the caviton continuum in the highest 2 to 4 range cells near reflection density. The most convincing proof of this identification is the much more rapid decay of the continuum spectrum following HF switch-off compared with the slower decay, on the collisional damping time scale, of the free mode and decay-cascade features which involve free LWs. The cavitons are heater driven, nonlinear excitations, which decay on a much faster collisionless damping time scale related to their small burnout dimensions of about 10-15 electron Debye lengths. The caviton continuum feature persisted in these experiments for the total duration of the heating pulse which varied from 5 ms to 50 ms. There is no altitude resolved data for longer heating times. Longer time, altitude integrated, data may be ambiguous because the caviton spectrum would appear as a (relatively) smooth background underlying a more discrete decay-cascade spectrum.

The observations of Fejer et.al. [1991] and Sulzer and Fejer [1994] showed that the free mode features in the height resolved spectra "disappeared" after 5 ms to 30 ms of heating

depending on the heater power and duty cycle. This 'disappearance' usually nearly coincided in time with the appearance of decay-cascade type spectra at lower heights. The altitude integrated observations of Cheung et.al. [1992] showed that the free mode features did not actually disappear but became broader in frequency and relatively much weaker than the spectrum for $\omega \leq \omega_{HF}$ which intensifies with the development of the strong decay-cascade type spectrum. The additional clutter introduced in higher altitude resolution bins due to this growing signal from lower altitudes would tend to obscure the free modes at these later times.

One to several ms after the continuum plus free mode spectra appeared in the upper altitude bins Sulzer and Fejer [1994] observed isolated free mode lines in the next one or two lower bins which were not accompanied by the caviton continuum. No 2D SLT simulations have been carried out to date in this intermediate density regime (between reflection and matching densities). Nearer to reflection density the free mode is always accompanied by the continuum. Further work is needed to see whether the isolated free mode is in disagreement with SLT predictions.

The decay-cascade type spectra are predicted to occur, in a smooth ionosphere, at altitudes at or below the matching height as shown in Fig. 2. The decay line results from the parametric decay of the heater into a LW and an IAW. The wave vector $\mathbf{k}_1$ of the most unstable waves corresponds to a peak in the modal energy spectrum $< |E(\mathbf{k})|^2 >$ and is determined from the decay frequency matching condition

$$\omega_{HF} = \omega_p(1 + \frac{3}{2}(k_1\lambda_D)^2) + k_1 c_s \tag{26}$$

and depends on the local electron density or plasma frequency ω_p. The radar observes only $k_1 = k_r$ and therefore sees only decay waves at a specific altitude (indicated by 1 in Fig. 2) which is slightly below the matching altitude (marked 0 in Fig. 2). The plasma line power spectrum $|E(\mathbf{k}_r,\omega)|^2$, in this case has a free LW peak at a frequency shifted by one IAW frequency, $k_r c_s$, below ω_{HF}. The cascade waves resulting from secondary and tertiary decay processes can satisfy the radar Bragg conditions at still lower altitudes and these have power spectra lying on the free mode dispersion curve lying about 3 $k_r c_s$ and 5 $k_r c_s$ below ω_{HF}. (These locations are marked 3 and 5 in Fig. 2.)

The decay and cascade modes appear as peaks in the modal energy spectra as shown in the lower right inset to Fig. 2. The positions of these peaks depend on $\omega_p(z)$, i.e. on altitude. Only at the heights indicated by 1, 3, 5 – in Fig. 2. do these peaks coincide with the wave vector, $\mathbf{k}_r$, observed by the radar. At these heights, $z_\nu(\nu = 1,3,5...)$, the power spectra, $< |\mathbf{E}(\mathbf{k}_r,\omega)|^2 >$, are sharp peaks at the free mode dispersion frequencies $\omega = \omega_p(z_\nu)(1 + \frac{3}{2}(k_r\lambda_D)^2) = \omega_{HF} - \nu k_1 c_s$ as shown DuBois et.al. [1993] for moderate heater powers characteristic of Arecibo experiments.

In the lower panels of Fig. 3 equal intensity contours are shown of the modal energy densities $< |E(\mathbf{k})|^2 >$ and $< |n(\mathbf{k})|^2 >$ in the decay-cascade regime obtained from 2D simulations of the SLT model. Distinct crescents associated with the decay and cascade steps are clearly seen. The angular width, away from the direction of $\mathbf{E}_0$ and $\mathbf{B}_0$ which are along k_x, is wider than the predictions [Fejer and Kuo 1973, Perkins et.al. 1974] based on the weak turbulence approximation (WTA) and consistent with the observations of decay and cascade structure at $\theta \sim 40°$ at Arecibo [DuBois et.al. 1993]. The number of cascade steps is generally significantly smaller for a given heater power than that predicted by the WTA [Hanssen et.al. 1992, DuBois et.al. 1993]. I now believe that there is an interesting

self-consistent physical connection between the number of cascade steps, the angular width of the spectrum and the "figure 8" structure seen in the lower right hand panel of Fig. 3, which has prominent perpendicular k components and is related to field aligned Langmuir filaments. This will be discussed in Section 5. It should be noted for this example that the strength of the geomagnetic field parameter, $1/2(\Omega_e/\omega_p)^2$, relative to the altitude parameter, $\Delta\Omega$ is typical of the matching height for the 933 Mhz radar at Tromsø.

In the observations of Sulzer and Fejer [1994] the earliest signal, about 1 ms or less after the onset of heating, was "below threshold spectrum" or a weak decay line originating near the matching height. (The matching height was accurately determined by extending the observed free mode line until it intersects $\omega = \omega_{HF}$.) It is reasonable that a below threshold spectrum is the first to be observed since it involves the beating of the heater with the ambient IAWs and does not require significant parametric growth. The caviton continuum plus free mode spectrum then appeared near reflection density about 1 ms or less later. In their experiments with 5 ms heater pulses no significant further development of spectra near matching height occurred. But for 50 ms heater pulses (950 ms between pulses) significantly enhanced decay or cascade spectra appeared at and above the matching height about 10 ms after the appearance of the continuum spectrum and about coincident in time with the disappearance of the free mode feature both at reflection height. The appearance of a strong decay-cascade spectrum at lower altitudes (but above matching height) coupled with the apparent disappearance of the free mode line at some tens of ms after the onset of heating was also characteristic of the earlier observations of Fejer et.al. [1991] and Cheung et.al. [1992]. It is generally agreed that these observations can be explained by the presence of density irregularities at these later times. In other words, the smooth layered ionosphere postulated in Fig. 2 is not consistent with the observations at these later times. I will discuss the effects of irregularities in Section 4. Crudely speaking, the irregularities scramble the altitude dependence of the electron density.

The older height integrated radar spectra [see e.g. Fejer et.al. 1985] are consistent with the above picture. These spectra generally consisted of decay-cascade type spectra sitting on a broad ($\omega < \omega_{HF}$) background.

The time behavior of the height resolved plasma line spectra are consistent with the earlier measurements Djuth, Sulzer and Elder [1990] of the altitude dependence of the total plasma line power as a function of time after the HF turn on in a unpreconditioned nighttime ionosphere. They found that for early times $t < t_s$, where t_s ranged from 30 ms to 100 ms with increasing HF power, the turbulence was concentrated in the Airy maximum nearest reflection height. For $t > t_s$ the turbulence spread to fill a height region between the reflection and matching heights. For times less than a few seconds the turbulence occurred in horizontal layers which coincided with the interference maxima of the heater. Sulzer and Fejer [1994] also observed this "Airy" layering. For longer times the turbulence retreats back to the reflection altitude and then breaks up into complex patches.

All the discussion above applies to radar spectra of HF induced turbulence observed at Arecibo at night. At Tromsø the observations [Stubbe et.al. 1992 a,b Djuth et.al. 1994] are significantly different. These differences and how they might be reconciled with the predictions of SLT theory are discussed in some detail in DuBois et.al. [1992, 1993]. One overall conclusion is that the ionosphere at Tromsø, at least during the observations of Djuth et.al. [1994a], contained density irregularities. The Tromsø observations, even after only a few ms of heating, look more like the long time or preconditioned ionosphere observations at Arecibo. The radar spectra are dominated by decay-cascade features on top of a broad continuous background. Kohl et.al. [1994] reported at this symposium the observation of

what might be interpreted as caviton continuum plus free mode spectra using the VHF radar at Tromsø.

I have not discussed the altitude dependence of the ion line spectra since such observations have not been made at Arecibo. We showed in DuBois et.al. [1993] on the basis of SLT simulations that the enhanced ion line intensity falls off faster with the increase of the angle between the radar observed $\mathbf{k}_r$ and the geomagnetic field than does the plasma line intensity. Therefore, the properties of the enhanced ion line seem harder to observe at Arecibo than at Tromsø where Djuth et.al. [1994a] observed the altitude dependence of the ion line spectra. These spectra often showed a pronounced peak centered at $\omega = 0$ in addition to the ion acoustic peaks at $\omega = \pm k_r c_s$ for both the UHF and VHF radars. We argued in DuBois et.al. [1992, 1993, 1994] that the $\omega = 0$ peak is a direct result of the nonresonant, low frequency density fluctuation driven by the impulsive ponderomotive force of the Langmuir field trapped in a collapsing caviton. These caviton features of the ion line spectrum again are most pronounced at densities approaching reflection density. Examples of computed ion line frequency spectra, $< |n(\mathbf{k}_r, \omega)|^2 >$, are shown in Fig. 4.

Using chirped radar techniques, Isham and Hagfors [1993] have measured the temporal and spatial distribution of the HF-induced Langmuir turbulence at Arecibo. The spectral resolution of their observations often could not distinguish between various predicted spectral signatures and most of their observations were in a preconditioned regime. In the nighttime ionosphere they observed rapidly changing regions of enhanced HFPLs spread over 3 km in height depending on heater power. These nighttime observations appear to be consistent with those of Djuth et. al [1990] and Sulzer and Fejer [1994], for example. The daytime observations of Isham and Hagfors showed that the HFPL originates about 200 m below the O mode reflection height within 20 ms of HF turn on and remains there for many seconds. A second region of enhanced HFPL was observed to form 1 to $\leq$ km below reflection height after 5 to 10 seconds of heating. They attributed the differences between day and night to increased D region absorption of the heater during daytime. Clearly, density irregularities must play a role in the daytime turbulence layer near reflection height if, as assumed by Isham and Hagfors, the plasma line spectrum is the decay-cascade type. Also the increased Landau damping of LWs due to higher daytime electron temperature cannot be dismissed because the $\mathbf{k}$ vector observed by the radar is relatively large.

Transient, upshifted plasma line features of several hundred kHz were observed by Isham et.al. [1990, 1994], using similar techniques with the UHF radar at Tromsø. These might be interpreted as solitary free mode lines similar to those observed by Sulzer and Fejer [1994] at Arecibo.

4. Speculations on Self-Consistent Theories of Langmuir Turbulence in Coexistence with Density Irregularities

There is overwhelming evidence, some of it discussed above, that the HF-induced Langmuir turbulence typically exists in an environment of density irregularities of various length scales. The exceptional case of a smooth ionosphere may only occur for the first tens of milliseconds in an unpreconditioned "cold start" at Arecibo. I have tried to list a hierarchy of irregularities which are thought to be important because of observations and/or theoretical predictions. My discussion is biased toward observations at Arecibo but some of these thoughts may apply to the auroral ionosphere as well. In listing possible density irregularities, I omit linear Langmuir and ion acoustic waves since these are well understood. If we start from the shortest spatial scales on up we can list:

I. Langmuir caviton density depletions. These have dimensions of 10 cm-50 cm ($10\lambda_{De}$ - $50\lambda_{De}$) created on time scales of .1 ms to .5 ms. (For these estimates I assume an ion sound speed of 1m/ms.) These are a familiar prediction of SLT theory, particularly near reflection density [DuBois et.al. 1988, 1990, 1991].

II. Langmuir filaments. These have transverse dimensions of 1 to 10 meters and are several times longer longitudinally and would take, say, 5 to 10 ms to form. A preliminary discussion of these will be a main topic of Section 5. They are also a direct prediction of the ponderomotive SLT model.

III. Horizontal density depletions. These are caused by the ponderomotive pressure of the induced turbulence at the heater interference maxima. They were discussed in DuBois et.al. [1993] and were estimated to have an altitude thickness of about 50 m and would take about 50 ms to form. A long delayed study is underway again in collaboration with Alfred Hanssen in which a large number of SLT simulations are carried out to determine the space and time averaged electric field energy density, $W(E_0, n_0) =< |E|^2 >$, as a function of heater intensity and mean electron density, n_0, in a homogeneous plasma. Since the scales of spatial variation of the heater field E_0 are much longer than turbulence correlation lengths the function $W(E_0(z), n_0(z))$ can be used to calculate the large scale ponderomotive or thermal density depletions caused by the layers of Langmuir turbulence which are localized at altitudes z near the heater standing wave maxima. The ponderomotive and thermal pressures of the electric fields of the Langmuir turbulence are typically an order of magnitude larger than those of the heater field itself near reflection density. Preliminary estimates are that density depletions of a few percent are possible in the first few heater maxima near reflection for typical heater powers. This program, when completed, should produce self-consistent, one dimensional, heater and induced turbulence profiles as a function of altitude z. The anomalous absorption of the heater as a function of altitude due to the parametric processes can also be included. Analogous calculations based on WTA estimates for the induced turbulence have been carried out by Vas'kov and Gurevich [1973] and DuBois and Goldman [1972].

It was argued in DuBois et.al. [1993] that these horizontal density depletions would produce new altitudes of matching densities, above the unperturbed matching height, where decay-cascade spectra could be observed by the Arecibo radar. This could occur on a time scale of 50 ms or less and could explain the longer time observations of Sulzer and Fejer [1994]. We also argued in Cheung et.al. [1992] and DuBois et.al. [1993] that these density depletions near reflection density would locally decrease the density scale length and broaden in frequency the free mode lines in the plasma line spectra from these altitudes.

Muldrew [1994 Comment] believes that field aligned density depletions or ducts (the SSFAIs discussed below) can also account for the observations. But I do not believe that any independent observational evidence or quantitative theory put forward to date can account for the formation of these ducts on such a short time scale [DuBois, 1994 Reply].

IV. Short scale field aligned irregularities (SSFAIs). These have been observed by radar scattering perpendicular to the geomagnetic field [Frey, 1980, Basu et.al. 1983]. Noble and Djuth [1990] have correlated 3 meter diameter SSFAIs with the excitation of the HF induced plasma line and Coster et.al. [1985] have estimated that these take a few seconds to develop after HF turn on perhaps indicating a developed length of about 1 km. Arce et.al. [1994], using an insitu rocket probe at the edge of the HF heated region, have observed such structures of about 8 m diameter, close packed in bundles of about 100 m wide with bundles separated by about 1 km. These structures are apparently related to the ducts

invoked by Muldrew [1978, 1988, 1992, 1994 Comment] to explain a variety of the observed properties of the HF induced turbulence. There are a number of competing theories for the formation of SSFAIs most of which involve thermally driven (Ohmic heating) processes. The thermal instabilities excited near HF reflection involve the nonlinear coupling of LWs generated by the PDI across geomagnetic field lines [Perkins, 1974; Lee and Fejer, 1978; Das et.al. 1983]. Instabilities driven at the upper hybrid resonance entail the coupling of HF-induced upper hybrid waves traveling across the magnetic field lines and/or the trapping of those waves in thermally induced density cavities; they include the thermal oscillating two stream instability [Grach et.al. 1977, 1978 a,b; Das and Fejer, 1979; Dysthe et.al. 1982, 1983; Mjlhus, 1983] the four wave thermal instability [Lee and Kuo, 1983] and the resonance instability [Vas'kov and Gurevich, 1975, 1977; Inhester et.al. 1981; Inhester, 1982]. These processes in the nonlinear limit might produce fully developed SSFAIs. The resonance instability requires finite amplitude "seed" irregularities to trigger nonlinear growth. The other processes or the Langmuir filaments, which I will discuss in Section 5, might provide this. Noble and Djuth [1990] argue that their observations of the correlation between SSFAIs and HF enhanced plasma lines imply that the Langmuir turbulence somehow provides the seeds for SSFAIs.

I will suggest in Section 5 that SLT theory in its simplest ponderomotive form might predict the filamentary seeds from which developed can SSFAIs grow.

V. Thermally driven heater filamentation or self-focusing. Thermal self-focusing of the heater can occur because a local fluctuation concentration of heater energy can cause a local temperature increase which causes hydrodynamic expansion. The concomitant increase in the local refractive index of the plasma concentrates the radiation in the heated region further increasing the heating. Thermal self-focusing has been studied by many workers [Perkins and Valeo 1974, Vas'kov and Gurevich 1977, Cragin et.al. 1977]. The theory of large scale HF-induced modifications is a closely related subject [e.g. Hansen et.al 1990]. The transverse dimension of the heater filaments tend to be on the order of a kilometers or somewhat less and they develop on times of several seconds.

The theories proposed to date have not taken into account the considerably enhanced thermal dissipation from the electric fields of the induced Langmuir turbulence. They have considered only the dissipation $\mathbf{E}_0 \cdot \underline{\underline{\sigma}} \cdot \mathbf{E}_0$ of the heater field $\mathbf{E}_0$ where $\underline{\underline{\sigma}}$ is the high frequency conductivity tensor. In fact the electric field energy density, $< |\mathbf{E}|^2 >= W(|\mathbf{E}_0|)$, of the Langmuir turbulence is typically an order of magnitude or so **higher** than that of the heater near reflection density and is a sensitive function of $|E_0|$. (See DuBois et.al. [1990], Hanssen et.al. [1992]). Thus at the heater interference maxima the thermal pressure (and the ponderomotive pressure) of the induced Langmuir fields can be far greater than that of the heater itself [Rose and DuBois, 1993, pages 3334-3355]. If we could ignore reflection and consider the heater as a plane traveling wave the enhancement effect of the turbulence can be shown to reduce the linear gain length for filamentation by a factor of $[1 + \partial W(|E_0|)/\partial |E_0|^2]^{-1}$ and to reduce the wavelength of the fastest growing transverse modulation by the square root of this factor. However, the existence of the reflection surface and the standing wave nature of the heater are essential for the ionosphere. The ohmic dissipation of the induced Langmuir turbulence would reduce the threshold for thermal filamentation as calculated by Cragin and Fejer [1974], accounting for the reflection surface, by about the same factor and therefore the horizontal wavelength of the marginally unstable mode would again be reduced by the same factor as above.

I believe that a more complete treatment of this problem should start from the horizontally layered self consistent pump and turbulence profiles discussed under 2., as an 'equi-

librium' state and then consider the stability of this state to horizontal (or magnetic field-transverse) perturbations. This remains to be carried out.

In the later stages of long HF pulse ($\sim$ CW) heating experiments or under preconditioned conditions to Arecibo the ionospheric state is probably very complex [Djuth et.al. 1990] – a state of "ionospheric mud" – as Frank Djuth has characterized it. In this state large and small scale irregularities may coexist in some fashion. It seems to me that the next challenge for hard, quantitative, theory is to study the induced turbulence in the 'early-intermediate' time interval, say a few hundred ms after the observed [Djuth et.al. 1990, Fejer et.al. 1992, Sulzer and Fejer 1994] drop of the turbulent zone below the reflection layer. In this time interval the horizontal stratifications and the SSFAIs should play a role. This is also the time interval of the "miniovershoot" [Showen et.al. 1977].

5. Does SLT Theory Predict the Seeds for Short Scale Field Aligned Irregularities?

In the low frequency density fluctuation model energy spectra, $< |n(\mathbf{k})|^2 >$, calculated in our earlier work [DuBois, et.al 1993 a, b, 1994 b], and in the examples shown in the lower right panel of Fig. 3, a "figure 8" structure appears with $k_x \simeq 0$ containing significant energy for perpendicular wave numbers $|k_y| > 0$. (Remember that heater field $\mathbf{E_0}$ is directed along $\mathbf{B_0}$ which is in the x direction.) This spectrum is consistent with the observations of SSFAIs such as the 49.92 MHz radar measurements of Noble and Djuth [1990]. The spectral density implies that in the turbulent field $n(x,y)$ there are narrow (in the perpendicular direction), field aligned structures. To visualize these structures we have taken the inverse Fourier transform including only those $\mathbf{k}$ modes which fall within the dashed box in Fig. 3 in the neighborhood of the "figure 8" structure. The contours for negative values of the resulting $n(x,y)$, i.e. density depletions are shown in the upper panel of Fig. 5. We indeed find field-aligned depletions, which we will call Langmuir filaments, even though they are more sausage-like than filamentary. For the frequency mismatch parameter $\Delta\tilde{\Omega}/w_p = 0.023$ which corresponds to the matching altitude for the Arecibo radar assuming $T_e \sim 0.1ev$ and a heater frequency of about 5 Mhz, these filaments are about 1 to 2 dimensionless units wide (in y) and about 10 units long (in x). The natural length unit is 3/2 $(\mathrm{M})^{1/2}\lambda_{D_e}$ where $M = m_i/\eta m_e$ where $\eta = 3.38$ for $T_e = T_i$ [DuBois et.al. 1994b]. Using $m_i/m_e \sim 6200$, which we used in our simulation, the filaments turn out to be about 1.0 m to 2.0 m wide and about 10 m long taking $\lambda_{D_e} \simeq 1\mathrm{cm}$.

We believe these filaments are the nonlinear saturated state in two dimensions of the transverse modulational or Langmuir filamentation instability studied recently by Rubenchik and Shapiro [1991, 1993]. They studied the stability of a one dimensional decay-cascade spectrum to modulations in the two transverse dimensions. The modulational instability of this spectrum evolved into collapsing, field-aligned, filaments in three dimensions. They made some simplifying assumptions such as infinitely long filaments in the field (our x) direction. Nevertheless, I believe their predictions are qualitatively correct. In our 2D simulations the filaments cannot undergo inertial (i.e. undriven) collapse since we have only one transverse dimension. In this case the system evolves into a set of soliton-like filamentary structures which are relatively long-lived. The absence of transverse filament collapse is a weakness of the 2D model. For stronger driving the filaments appear to shrink or break up in the x direction and undergo 2D collapse similar to the collapse which we observe near reflection density. It remains to be studied whether this is an artifact of 2D; in 3D the transverse filament or sausage-like collapse may dominate the longitudinal or pancake-like collapse. Near reflection density we typically see pancake-like collapsing cavitons which are shorter in the x dimension than in the y dimension [DuBois et.al. 1990]. Our conjecture

is that in 3D we have pancake-like collapsing cavitons near reflection density and sausage-like collapsing filaments at lower densities, closer to matching density. The results provide a strong incentive to carry out fully 3D simulations which are probably only possible, in the parameter ranges of interest, on the new massively parallel computers. Some related results were published by Newman and Goldman [1992]. They solved the same dynamical equations in 2D and 3D for parameters in the cavitation regime **near reflection density**. In the absence of a background magnetic field they found that in a time averaged sense the collapsing cavitons lay in $\mathbf{E}_0$ aligned density channels whereas for $\Omega_e/\omega_p = 0.3$ they lay in nearly **perpendicular** channels.

We can make some analytic estimates based on the properties of the computed $\mathbf{k}$ spectra to the computed spatial structures. We can generally express the potential $\Psi(x,y)$ of the Langmuir envelope field ($\mathbf{E} = \nabla\Psi$) as

$$\Psi(x,y,t) = \sum_{\nu}\sum_{\mathbf{k}} |\Psi_\nu(\mathbf{k})| e^{i\psi_\nu(\mathbf{k})} e^{ik_x x} e^{ik_y y} e^{-ik^2 t} \tag{27}$$

where there is a discrete sum over ν enumerating the decay-cascade crescents (seen for example in the lower left panel of Fig. 3) and there is a sum over $\mathbf{k}$, the 2D $\mathbf{k}$ space. Let ν run over positive and negative integers where Fig. 3d implies the symmetry $k_\nu = -k_{-\nu}$. Consistent with our computed power spectra and zero or weak geomagnetic field we assume that the Langmuir frequencies have the free-mode dispersion $\omega = k^2$ (in our scaled units) relative to the local plasma frequency. We can compute the equal time correlation function

$$\begin{aligned} \mathbf{C}_{\psi\psi^*}(x-x', y-y') &= \langle \Psi(x,y)\Psi^*(x',y') \rangle \\ &= \sum_{k,\nu} \langle |\Psi_\nu(k)|^2 \rangle e^{ik_x(x-x')} e^{ik_y(y-y')} \end{aligned} \tag{28}$$

the brackets represent an ensemble or time average and I have assumed random or uncorrelated phases

$$\langle e^{i[\psi_\nu(\mathbf{k}) - \psi_{\nu'}(\mathbf{k}')]} \rangle = \delta_{\nu\nu'}\delta_{\mathbf{k},\mathbf{k}'} \tag{29}$$

The later assumption appears justified for modes within a given crescent ν which grow independently from random noise. Next we introduce an ansatz based on the shape of the calculated spectra

$$|\Psi_\nu(\mathbf{k})|^2 = |\Psi_\nu(k,\theta)|^2 = (2\pi)^{3/2} \frac{\overline{U}_\nu}{\overline{\theta}_\nu} \delta(k-k_\nu) \; exp \; (-\theta^2/2\overline{\theta}_\nu^2) \tag{30}$$

where k and θ are the cylindrical coordinates in k_x, k_y space and k_ν is the radial location of the ν^{th} narrow crescent and $\overline{\theta}_\nu$ a measure of its angular width. This ansatz is valid for a weak background magnetic field. Here $\overline{W}_\nu = \int d^2k k^2 |\Psi_\nu(k)|^2 = k^2 \overline{U}_\nu$ is the spectral energy in the ν^{th} crescent. If we convert from a sum over $\mathbf{k}$'s to an integral over k and θ and make the small angle assumption $\overline{\theta}_\nu \ll 1$ we easily find for the correlation function with $x' = y' = 0$,

$$C_{\psi\psi^*}(x,y) = \sum_{\nu>0} e^{ik_\nu x} \frac{2\overline{U}_\nu \cos k_\nu x}{(1+ix/\Lambda_\parallel)^{1/2}} \; exp \; \left[\frac{-(y/\Lambda_\perp)^2}{2(1+ix/\Lambda_\parallel)} \right], \tag{31}$$

where the transverse and longitudinal scale lengths (which in general depend on ν) are

$$\Lambda_\perp = \frac{1}{k_\nu \overline{\theta}_\nu} \equiv \frac{1}{\Delta k_\perp} \tag{32a}$$

$$\Lambda_{\|} = \frac{1}{k_\nu \overline{\theta}_\nu^2} \equiv \frac{k_\nu}{(\Delta k_\perp)^2} \tag{32b}$$

I have used the $\nu \rightarrow -\nu$ symmetries: $k_{-\nu} = -k_\nu$ and $\overline{U}_\nu = \overline{U}_{-\nu}$ so that in this expression ν is summed only over positive integers. The angular width of calculated spectra can roughly be fitted with $\overline{\theta}_\nu \sim 0.3$ so that $\Lambda_{\|} \sim 3\Lambda_\perp$. In 3D it can be seen that the major qualitative change is that the square root in the denominator in (31) is replaced by the first power giving a more rapid fall off in x.

With the random phase assumption $\Psi(x,y)$ is a (complex) Gaussian random field. We can apply the methods developed by colleague Harvey Rose [Rose and DuBois 1992, 1993] to study the statistics and filamentation of laser beams processed by random phase plates. This work relys on two theorems of Adler [1981] on the properties of maxima or minima of real Gaussian fields. One of these theorems allows us to predict the probability distribution of the intensities of maxima which are much more probable than a naive Gaussian distribution.

The second theorem, which is more relevant for the present discussion, leads to the result that the amplitude and phase of the potential field in the neighborhood of a maximum in $|\Psi(x,y)|$ can be expressed deterministically, apart from an arbitrary phase, in terms of the correlations function

$$\Psi(x,y,t)_{max} = \Psi(o,o,t)\frac{C_{\psi,\psi^*}(x,y,t)}{C_{\psi,\psi^*}(o,o)} \tag{33}$$

where $C_{\psi,\psi^*}(o,o,t) = \langle|\Psi|^2\rangle = \sum_\nu \overline{U}_\nu$ and $\Psi(o,o,t)$ is a complex function of t expressing the value of $\Psi(x,y,t)$ at its extremum which we take to be $x = y = 0$. Thus, the shape of the potential near the extremum is actually determined by the correlation function. In the neighborhood of $x = y = 0$ the spatial derivatives must also be large since we are assuming an intense extremum. Hence, we can obtain expressions for the intense electric fields in the neighborhood of this extremum by taking the gradient of (33) using (31) and (32). With these we can compute the low frequency density depletions or minima caused by the ponderomotive pressure of these field extrema:

$$n(x,y)_{min} = -|\nabla\Psi(x,y)_{max}|^2. \tag{34}$$

If (31)-(33) are used to compute this it is found that

$$|\nabla\Psi(x,t)|^2_{max} \approx \frac{|\Psi(o,o,t)|^2}{\langle|\Psi(t)|^2\rangle}\frac{1}{(1+x^2/\Lambda_{\|}^2)^{1/2}} \quad \exp\left[\frac{-(y/\Lambda_\perp)^2}{(1+x^2/\Lambda_{\|}^2)}\right]$$

$$4\sum_{\nu\nu'>0}\left[k_\nu k_{\nu'} + \frac{1}{\Lambda_\perp^2}\frac{(y/\Lambda_\perp)^2}{(1+x^2/\Lambda_{\|}^2)}\right]\overline{U}_\nu\overline{U}_{\nu'}\cos k_{\nu'}x\cos k_{\nu'}x \tag{35}$$

where I have made the additional simplifying assumptions that the $\Lambda_{\|}$ and $\Lambda_\perp$ are the same for all ν and that $k_\nu\Lambda_{\|} = (k_\nu/\Delta k_\perp)^2 \gg 1$. To make contact with the density depletion structures observed in Fig. 6a it is necessary to filter out the higher k_x components in (35) which lie outside the dashed box region in Fig. 3. This effectively replaces the factor $\cos k_\nu x \cos k_{\nu'}x$ in (35) by the modulation $(1/2)\cos[(k_\nu - k_{\nu'})x]$ where $k_\nu - k_{\nu'} = (\nu-\nu')k* \equiv (\nu-\nu')(2/3)(m_e/m_i)^{1/2}k_D$. This factor modulates an overall shape which is consistent with the Langmuir filaments obtained in Fig. 6 having a slow fall-off in x on the scale of $\Lambda_{\|}$ and a more rapid, Gaussian fall-off in y on the scale of $\Lambda_\perp \sim 1/3\Lambda_{\|}$.

Comparing (31) to (35) we then see that the cascade-decay LWs are confined to the filamentary region of density depletion. This confinement self-consistently leads to the broadening of the Langmuir spectrum – i.e. to finite $\Delta k_\perp$ – allowing the decay-cascade features to be observed at radar k vectors making an angle as large as 45° with $\mathbf{E}_0$ or $\mathbf{B}_0$. This picture is verified in the lower panel of Fig. 5 where $|E(x,y)|^2$ is constructed only from the modes (within the dotted lines) in the outer two crescents ($\nu = \pm 1$) in Fig. 3. To make contact with the $|E(x,y,t)|^2$ structures shown in the lower panel of Fig. 6 only the $\nu = \nu' = 1$ form should be kep in (35), consistent with the modes cut in Fig. 3. In this case the overall shape factor is modulated by the standing wave $\cos^2 k_1 x$ in agreement with the observed pattern in Fig. 6. Comparison of the upper and lower panels of Fig. 5 shows that intense standing Langmuir wave trains are mostly confined to the deepest density throughs. The complete spatial dependence arising from the sum over ν is similar but more complex and difficult to display graphically. We also find that the decay-cascade IAWs are similarly confined which is consistent with the broad (in k_y) decay-cascade crescents in the $\langle |n(\mathbf{k})|^2 \rangle$ spectra in Fig. 3. The lack of a complete correlation between the density channels and the electric field standing wave trains may be due to the ion inertia which delays the response of the density to the ponderomotive force.

Thus, these self-consistently created Langmuir filaments may partly fullfill the role of the field aligned ducts postulated by Muldrew [1978-1994]. In SLT theory they arise as a natural part of the induced Langmuir turbulence. They appear to arise on roughly the same time scale as the decay-cascade spectra. Are these the seeds for the SSFAIs which Noble and Sulzer [1990] inferred from their observations?

Note that the longitudinal dimensions (in x) of these filaments appear to be too short for thermal effects to be strong – i.e. the electron thermal conductivity along the field lines is too large to build up a strong local temperature increase. However, since these lengths are much less than the electron collisional mean free paths ($\gtrsim$ 200 m) the classical Spitzer-Harm thermal conductivity should not be used but instead a reduced k dependent, non-local thermal conductivity such as studied in the laser fusion context [e.g. Epperlein et.al. 1990]. My estimates indicate that thermal effects are not important even using the reduced thermal conductivities of Epperlein [1990] for an unmagnetized plasma. The latter, however, have not been calculated in the same magnetic field geometry needed for the ionosphere. Conceivably on a longer time scale with thermal effects taken into account these short Langmuir filaments might merge into longer field aligned filaments.

The truncation in the observed number of cascade stops as compared to WTA estimates is consistent with the additional collisional stabilization resulting from additional Langmuir modes resulting from this spreading in $k_\perp$. I would expect all of these effects to be accentuated in 3D because the possibility of filament collapse should lead to even greater confinement and a broader spectrum in $k_\perp$ and probably significant collisionless damping which terminates the collapse. This greater confinement may be countered by the magnetic term in the LW dispersion relation. Further simulations with larger alues of $\Omega e/\omega_p$ than used is the example gien here will be needed to understand this.

An obvious technical question to ask about these field aligned structures in our simulations is their consistency with the known inaccuracy, mentioned in Section 2 and in DuBois et.al. [1994b], of the ion density response $D(\mathbf{k},\omega)$ [see (17)] for $k_x = 0, k_y \neq 0$. We have computed the power spectra, $\langle |n(k_x = 0, k_y; \omega|^2 \rangle$, which show that the spectral energy is concentrated at $\omega \ll k_\perp c_s \sim k_\perp v_i$ where in fact $D(\mathbf{k},\omega)$ is accurately modelled in our simulations.

It is likely, then, that SLT theory is even richer than we had previously understood. It seems to contain a self-consistent, nonlinear relationship between the decay-cascade process and Langmuir filaments which may be the seeds for short scale field aligned irregularities.

6. Summary and Conclusions

In summary I believe the unpreconditioned observations at Arecito, culminating in the observations of Sulzer and Fejer [1994], justify the following statement: SLT theory describes, in quantitative detail, the early-time, non-preconditioned, observations at Arecibo. This is the **only** case in which we can be quite confident that we know the plasma conditions; (for example, we know [Djuth et.al. 1994b] that the unpreconditioned electron density profile is smooth with $\delta n/n_0 < 10^{-3}$, which is smaller than the thermal dispersion of the observed LWs and, therefore, will not significantly perturb the matching altitudes.) In this early time regime the conventional WTA theory fails completely.

The one remaining caveat to this statement, in my opinion, is that the isolated free mode observed by Sulzer and Fejer [1994] has not yet been predicted by SLT theory. Simulation power spectra in the relevant density regime, however, have yet to be carried out.

Now if the above statement is provisionally accepted, it seems only reasonable to me to explore the predictions of SLT theory in more complex regimes. The preconditioned or later-heating-time ionosphere at Arecibo is almost universally expected to contain density irregularities. I have briefly discussed how horizontally stratified density depletions might arise from the ponderomotive pressure of the intense layers of Langmuir turbulence concentrated at the heater interference maxima. This could explain the occurrence [Sulzer and Fejer, 1994] of decay-cascade matching altitudes above the unpreconditioned matching altitudes as well as the broadening or apparent drop-out of the free-mode line at later heating times. At later heating times the velocity distribution of electrons will also be altered by the turbulence. Heating of the distribution – either bulk heating or hot electron tails – will tend to weaken the turbulence and this may be related to observed "overshoots" in the HFPL power. Such phenomena are complex, self-consistent, nonlinear problems which are in need of detailed study. SLT theory has not been adequately or correctly applied to the late time or preconditioned regimes because of the great technical difficulties in doing so. If there is a competing theory, that is physically and theoretically sound, which can describe all of these phenomena more accurately than does SLT theory, it has yet to be revealed.

The comparison of SLT theory with the Tromsø observations has been less clear. The early time continuum plus free mode signatures, which are consistently observed in the unpreconditioned ionosphere at Arecibo, did not often appear at Tromsø, although Fig. 10 of Kohl et.al. [1993] seems an exception. The recent time and height resolved, VHF radar observations of Kohl et.al. [1994], announced at this Symposium, appear to show the continuum plus free mode signatures at a higher altitude than the decay-cascade type spectra. This is consistent both with Arecibo observations and with SLT predictions. Reasons why these signatures are move easily observed at Arecibo are discussed in Hanssen et.al. [1992], DuBois et.al. [1993] and by Sulzer and Fejer [1994]. For example, SLT simulations predict [Cheung et.al. 1992], in agreement with observations, that the free-mode may not be observed for the 430 MHz Arecibo radar with a heater frequency of 3.175 MHz or with the 933 MHz Tromsø radar with a heater frequency of 6 MHz (assuming $T_e \sim 1000°K$) because of the relatively strong Landau damping of the observed Langmuir waves. If the electron temperature is initially somewhat lower, a transient appearance of the free mode might occur, in these cases, until local heating again increases the Landau damping. The unpreconditioned ionosphere at Tromsø may be typically noisier

at Tromsø than at Arecibo so that natural irregularities at Tromsø may complicate the comparison of theory and observations. Some of the diagnostics used by Sulzer and Fejer [1994] have not been implemented at Tromsø. For example, a precise determination of the

matching altitude by extrapolating the free mode lines has not been made. It is clear that the altitude spread of the cascade decay spectra observed by Djuth et.al. [1994a] can only be understood if density irregularities of a few percent are present during the observations. Therefore, the Tromsø environment in this case may be as complex as the late time or preconditioned environment at Arecibo. I mentioned the $\omega = 0$ feature often present in the Tromsø ion line data, for both VHF and UHF radars, as a signature of Langmmuir collapse. In some cases, particularly for the UHF radar, a sharp $\omega = 0$ ion line is seen along with a sharp "OTSI" line in the plasma line spectrum. In other cases a broader $\omega = 0$ ion line feature is seen without the OTSI feature. The later case is more consistent with most SLT simulations. However, several workers [Sprague and Fejer, 1994, Glanz et.al. 1993, and Alfred Hanssen, 1993, private communication] have observed sharp OTSI lines in SLT simulations under special conditions of weak pumps and strong ion acoustic wave damping. It remains a challenge to reconcile these predictions with the Tromsø observations.

The fundamental basis of SLT models appears to me to be sound for the conditions of hf heating. For the strongest heater powers of projected facilities such as HAARP the small parameter ordering necessary for such models (and discussed in Section 2) may break down provided the high heater power actually reaches the F region without absorption. The recent kinetic theory studies outlined in Section 2 are the basis for these statements. To understand the late heating time predictions of these models, there remains much to do in studying the global and local deformation of the electron and ion velocity distributions as the turbulence evolves. The usual isothermal approximation is certainly not valid as the turbulence develops.

The main new theoretical result presented here concerns the self-consistent generation of Langmuir filaments in the decay-cascade regimes. We find that the LWs and IAWs participating in the decay-cascade processes are confined to relatively short, field aligned density channels. More research is needed to understand how these structures scale with density, magnetic field and pump power. These remains the intriging possibility that these filaments are the seeds for short scale field aligned irregularities.

Most of my SLT research discussed above was carried out in collaboration with my colleagues, David Russell and Harvey Rose, who also made important suggestions which improved this paper.

I have also profited from conversations with Frank Djuth, Jules Fejer, Martin Goldman, Alfred Hanssen, Erlend Helmerson, Einar Mjølhus, and Mike Rietveld.

This work was supported by the USDOE.

References

Adler, J., The geometry of random fields, *Wiley*, New York, 1981.

Basu, S., S. Ganguly, and W. E. Gordon, Coordinated study of subkilometer and 3-m irregularities in the F region generated by high power HF heating at Arecibo, *J. Geophys. Res.* **88**, 9217-9225, 1983.

Bezzerides, B., D. F. DuBois and D. W. Forslund, Magnetic field generation by resonance absorption of light, *Phys. Rev.* **A16**, 1678, 1977.

Carlson, H. C., W. E. Gordon, and R. L. Showen, High-frequency induced enhancements of incoherent scatter spectrum at Arecibo, *J. Geophys. Res.* **77**, 1242, 1972.

Cheung, P. Y., A. Y. Wong, T. Tanikawa, J. Santoru, D. F. DuBois, H. A. Rose, and D. Russell, Short-time-scale evidence for strong langmuir turbulence during hf heating of the ionosphere, *Phys. Rev. Lett.* **62**, 2676, 1989.

Cheung, P. Y., D. F. DuBois, T. Fukuchi, K. Kawan, H. A. Rose, D. Russell, T. Tanikawa and A. Y. Wong, Investigation of strong Langmuir turbulence in ionospheric modification, *J. Geophys. Res.* **97**, 10, 575, 1992.

Coster, A. J., F. T. Djuth, R. J. Jast and W. E. Gordon, The temporal evolution of three-meter striations in the modified ionosphere, *J. Geophys. Res.* **90**, 2807-2818, 1985.

Cragin, B. L., and J. A. Fejer, Generation of large scale-field aligned irregularities in ionspheric modification experiments, *Radio Sci.* **9**, 1071-10-75, 1974.

Cragin, B. L., J. A. Fejer and E. Leer, Generation of artificial spread F by a collisionally coupled purely growing parametric instability, *Radio Sci.* **12**, 273, 1977.

Das, A. C., and J. A. Fejer, Resonance instability of small scale field aligned irregularities, *J. Geophys. Res.* **84**, 6701-6704, 1979.

Djuth, T. F., C. A. Gonzales, and H. M Ierkic, Temporal evolution of the HF-enhanced plasma line in the Arecibo *F* region, *J. Geophys. Res.* **91**, 12,089, 1986.

Djuth, F. T., M. P. Sulzer, and J. H. Elder, High-resolution observations of the HF-induced plasma waves in the ionosphere, *Geophys. Res. Lett.* **17** , 1893, 1990.

Djuth, F. T., P. Stubbe, M. P. Sulzer, H. Kohl, M. T. Rietveld, and J. H. Elder, Altitude characteristics of plasma turbulence excited with the Tromsø superheater, *Geophys. Res. Lett.* **99**, 333-339, 1994a.

Djuth, F. T., M. P. Sulzer, and J. H. Elder, Application of the coded long-pulse technique to plasms line studies of the ionosphere, *Geophys. Res. Lett.* in press, 1994b.

DuBois, D. F., and M. V. Goldman, Radiation-induced instability of electron plasma oscillations, *Phys. Rev. Lett.* **14**, 544, 1965.

DuBois, D. F., and M. V. Goldman, Nonlinear saturation of the parametric instability: Basic theory and applications to the ionosphere, *Phys. Fluids* **15**, 919, 1972.

DuBois, D. F., A. Hanssen, and H. A. Rose, Comment on "Langmuir turbulence and ionospheric modification," by P. Stubbe, H. Kohl and M. T. Rietveld, *J. Geophys. Res.* **97**, 15,059, 1992.

DuBois, D. F., A. Hanssen, H. A. Rose, and D. Russell, "Excitation of strong-Langmuir turbulence in the ionosphere: Comparison of theory and experiment," *Phys. Fluids B* **5**,

26165, 1993.

DuBois, D. F., A. Hanssen, H. A. Rose, and D. Russell, Space and time distribution of HF excited Langmuir turbulence in the ionosphere: Comparison theory and observations, *J. Geophys. Res.* **98**, 17,543-17,567, 1993.

DuBois, D. F., Reply to the Comments by D. B. Muldrew, *J. Geophys. Res.* **99**, 15093-15095, 1994a.

DuBois, D. F., D. Russell and H. A. Rose, Reduced description of strong Langmuir turbulence from kinetic theory, *submitted to Physics of Plasmas*, 1994b.

Dysthe, K. B., E. Mjolhus, H. L. Pécseli, and K. Rypdal, Thermal cavitons, *Phys. Sci.* **T2/2**, 548-559, 1982.

Dysthe, K. B., E. Mjolhus, H. L. Pécseli, and K. Rypdal, A thermal oscillating two-stream instability, *Phys, Fluids* **26**, 146-157, 1983.

Epperlein, E. M., Kinetic theory of laser filamentation in plasmas, *Phys. Rev. Lett.* **65**, 2145, 1990.

Fejer, J. A., and Y. -Y. Kuo, Structure in the nonlinear saturation spectrum of parametric instabilities, *Phys. Fluids* **16**, 1490, 1973.

Fejer, J. A., M. P. Sulzer, and F. T. Djuth, Height dependence of the observed spectrum of radar backscatter from HF-induced ionospheric turbulence, *J. Geophys. Res.* **96**, 15,985, 1991.

Frey, A., Artificially produced field-aligned short-scale striations, M. S. Thesis, Rice University, Houston, TX, 1980.

Gavrilov, E., D. F. DuBois, H. A. Rose and A. M. Rubenchik, Resonance absorption evolution into Langmuir turbulence, *Computer Phys. Comm.* **81**, 65-73, 1994.

Glanz, J., M. V. Goldman, D. L. Newman, and C. J. McKinstrie, Electromagnetic instability and emission from counterpropapating Langmuir waves, *Phys. Fluids* **85**, 1101, 1993.

Goldman, M.V. D., L. Newman and F. W. Perkins, Fluid closures which mimic wave-particle interactions in strong Langmuir turbulence, *Phys. Rev. Lett.* **70**, 647, 1993.

Goodman, S., Strong turbulence equations derived from kinetic theory, *Phys. Fluids* **B4**, 329-335, 1992.

Grach, S. M., A. N. Karasktin, N. A. Mityokov, V. O. Rapoport, and V. Yu Trakhtengerts, Parametric interaction between electromagnetic radiation and ionospheric plasma, *Radiophys. Quantum Electron.*, Engl. Transl., **20**, 1254-1258, 1977.

Grach, S. M., A. N. Karasktin, N. A. Mityokov, V. O. Rapoport, and V. Yu Trakhtengerts, Theory of the thermal parametric instability in an inhomogeneous plasma, *Sov J. Plasma Phys.*, Engl. Transl. **4**, 737-741, 1978a.

Grach, S. M., A. N. Karasktin, N. A. Mityokov, V. O. Rapoport, and V. Yu Trakhtengerts, Thermal parametric instability in an inhomogeneous plasma (nonlinear theory), *Sov. J. Plasma Phys.*, Engl. Transl. **4**, 742-747, 1978b.

Gurevich, A. V., Y. S. Dimant, G. M. Milikk and V. V. Vas'kov, Multiple accelerration of electrons in the regions of high power radio-wave reflections in the ionosphere, *J. of Atmos. Terr. Phys.* **44**, 1089, 1985.

Hammett, G. W., and F. W. Perkins, Fluid moment models for landau damping with application to the ion-temperature-gradient instability, *Phys. Rev. Lett.* **64**, 3019, 1990.

Hanssen, J. D., G. J. Morales, L. M. Duncan, J. E. Maggs, and G. Dimonte, Large-scale ionospheric modifications produced by nonlinear refraction of an HF wave, *Phys. Rev. Lett.* **65**, 3285, 1990.

Hansen, A., E. Mjølhus, D. F. DuBois, and H. A. Rose, Numerical test of the weak turbulence approximation to ionospheric Langmuir turbulence, *J. Geophys. Res.* **97**, 12,073, 1992.

Helmersen, E., and E. Mjølhus, A semikinetic model for ionospheric Langmuir turbulence, *J. Geophys. Res.* **99**, 17623-17629, 1994.

Inhester, B., A. C. Das, and J. A. Fejer, Generation of small scale field aligned irregularities in ionospheric heating experiments, *J. Geophys. Res.* **86**, 9101-9106, 1981.

Isham, B., and T. Hagfors, Observations of the temporal and spatial deelopment of HF-enhanced plasma lines at Arecibo using chirped ISR, *J. Geophys. Res.* **98**, 13605, 1993.

Isham, B., C. LaHaz, T. Hagfors, H. Kokl, T. B. Leyser, and M. T. Rietveld, Recent EISCAT heating results using chirped ISR, paper at IV Suzdal URSI Symposium on Artificial Modification of the Ionosphere, Uppsala, Sweden, August 15-20, 1994.

Kohl, H., H. Kopka, P. Stubbe, ad M. T. Rietveld, Introduction to ionospheric heating experiments at Tromsø-II scientific problems, *J. Atm. and Terr. Phys.* **55**, 601, 1993.

Kohl, H., M. T. Rietveld, B. Isham, and C. LaHoz, Spectra of heater induced Langmuir turbulence with high altitude resolution, IV Suzdal URSI Symposium on artificial modification of the ionosphere, Uppsala, Sweden, August 15-20, 1994.

Lee, M. C., and J. A. Fejer, Theory of short-scale field aligned density striations due to ionospheric heating, *Radio Sci.* **13**, 893-899, 1978.

Lee, M. C., and S. P. Kuo, Excitation of upper hybrid waves by a thermal parametric instability, *J. Plasma Phys.* **30**, 463-478, 1983.

Mjølhus, E., On reflexion and trapping of upper hybrid waves, *J. Plasma Phys.* **29**, 195-215, 1983.

Muldrew, D. B., The role of field-aligned ionization irregularities in the generation of HF-induced plasma lines at Arecibo, *J. Geophys. Res.* **82**, 2552, 1978.

Muldrew, D. B., Duct model explanation of the plasma line overshoot observed at Arecibo, *J. Geophys. Res.* **93**, 7598, 1988.

Muldrew, D. B., Duct model for the duty-cycle variation of the plasma-line overshoot during cyclic heating at Arecibo, *AGARD Conf. Proc.* **485**, 11A -1-11A-6, 1991a.

Muldrew, D. B., Duct model explanation of the broad component of the plasma-line spectrum observed at Arecibo, *Geophys. Res. Lett.* **18**, 2289, 1991b.

Muldrew, D. B., Initial duct growth determined from cold-start plasma-line spectra observed at Arecibo, *Geophys., Res. Lett.* **19**, 65, 1992.

Muldrew, D. B., Commenta on "Space and time distribution of HF excited Langmuir turbulence in the ionosphere: Comparison of theory and experiment" by DuBois et.al., *J. Geophys. Res.* **99**, 15,087-15,092, 1994.

Newman, D. L. and M. V. Goldman, Ionospheric turbulence driven by an electromagnetic pump below the upper-hybrid frequency, in Nonlinear Processes in Physics, A. S. Fokas et.al. editors, pp. 18–184, Springer-Verlag 1993.

Noble, S. T., and F. T. Djuth, Simultaneous measurements of HF-enhanced plasma waves and artificial feild-aligned irregularities at Arecibo, *J. Geophys. Res.* **95**, 15,185-15,207, 1990.

Perkins, F. W. and P. K. Kaw, On the role of plasma instabilities in ionospheric heating by radio waves, *J. Geophys. Res.* **76**, 282, 1971.

Perkins, F. W., A theoretical model for short-scale field-aligned plasma density striations, *Radio Sci.* **9**, 1065-1070, 1974.

Perkins, F. W., C. Oberman, and E. J. Valeo, Parametric instabilities and ionospheric modification, *J. Geophys., Res.* **79**, 1478, 1974.

Perkins, F. W., and E. J. Valeo, Thermal self-focusing of electromagnetic waves in plasmas, *Phys. Rev. Lett.* **32**, 1234-1237, 1974.

Rietveld, M. T¿, H. Kokl, and N. P. Goncharov, Recent results using EISCAT's heating facility at Tronsø, keynote paper, IV Suzdal URSI Symposium on Artificial Modification of the Ionosphere, August 15-20, 1994, Uppsala, Sweden.

Rose, H. A., and D. F. DuBois, Initial development of ponderomotive filaments in plasma from intense hot spots produced by a random phase plate, *Phys. Fluids B* **5**, 3337, 1993.

Rubenchik, A. M., and E. G. Shapiro, Langmuir turbulence at low pumping levels, *Sov. Phys. JETP* **75**, 48-56, 1993.

Rubenchik, A. M., and E. G. Shapiro, Coexistence of weak and strong Langmuir turbulence, *JETP Lett.*, Engl. Transl., **54**, 17-21, 1991.

Showen, R. L., Time variation of the HF induced plasma waves, Ph.D. Thesis, Rice

University, Houston, TX, 1975.

Showen, R. L., and D. M. Kim, Time variations of HF-induced plasma waves, *J. Geophys. Res.* **83**, 623, 1978.

Stubbe, P., The concept of a kinetic transport theory, *Phys. Fluids* **B2**, 22-23, 1990.

Stubbe, P., H. Kohl, and M. T. Rietveld, Langmuir turbulence and ionospheric modification, *J. Geophys. Res.* **97**, 6285, 1992a.

Stubbe, P., H. Kohl, and M. T. Rietveld, Reply, *J. Geophys. Res.* **97**, 15067, 1992b.

Sulzer, M. P. and J. A. Fejer, Radar spectral observations of HF-induced ionospheric Langmuir turbulence with improved range and time resolution, *J. Geophys. Res.* **99**, 15035-15050, 1994.

Vas'kov, V. V., and A. V. Gurevich, Self-action of radio waves in the vicinity of plasma resonance, *Sov. Phys. JETP,* Engl. Trans., **37** 646, 1973.

Vas'kov, V. V., and A. V. Gurevich, Nonlinear resonant instability of a plasma in the field of an oridnary electromagnetic wave, *Sov. Phys. JETP*, Engl. Transl., **42**, 91-97, 1975.

Vas'kov, V. V., and A. V. Gurevich, Resonance instability of small-scale plasma perturbations, *Sov. Phys. JETP*, Engl. Transl., **46**, 487-494, 1977.

Vas'kov, V. V., and A. V. Gurevich, Staturation of self-focusing instability for radio wave beams in plasma, *Sov. J. Plasma Phys.* **3**, 185, 197.

Wang, J. G. -I-D Vlasov simulations of strong Langmuir turbulence in a radiation driven plasma, Ph.D. Thesis, University of Iowa, December 1993.

Wang, J. G., G. L. Payne, D. F. DuBois and H. A. Rose, One dimenstional simulations of Langmuir collapse in a radiation driven plasma, *Phys. of Plasmas*, in press, 1994.

Wong, A. Y., and R. J. Taylor, Parametric excitation in the ionosphere, *Phys. Rev. Lett.* **27**, 644, 1971.

Zakharov, V. E., Collapse of langmuir waves, *Sov. Phys. JETP*, Engl. Transl., **35**, 908, 1972.

Figure Captions

Fig. 1 Results from 1D Vlasov simulation of J. G. Wang [1993] with $W_0 = |E_0|^2/16\pi n_0 Te = 3.125 \times 10^{-2}, \omega_0 = \omega_{p_e}, T_e = T_i, m_i/m_e = 1836$. Upper left: envelope of Langmuir field showing a caviton near its maximum amplitude. Lower left: the ion density at the same time. Upper right: the electron phase space and Lower right: the ion phase space.

Fig. 2 Schematic figure showing the altitude distribution of different regimes of HF induced Langmuir turbulence in a ionospheric density profile monotonically increasing with altitude. Altitude is increasing vertically and the horizontal axis is the angular frequency ω. Inset boxes along the $\omega = \omega_{HF}$ (heater frequency) line are plasma line power spectra, proportional to $|E(\mathbf{k}_r, \omega)|^2$, at different altitudes. Any power spectral feature measured by the radar at $\mathbf{k} = \mathbf{k}_r$ associated with a free Langmuir wave must lie along the free mode dispersion line $\omega_L(k_r, Z)$. The inset boxes on the right side of the figure are modal energy spectra, $\langle |E(\mathbf{k})|^2 \rangle$, for different altitude slices. The radar "sees" only the $\mathbf{k} = \mathbf{k}_4$ component. From DuBois et.al. [1993].

Fig. 3 Time averaged modal energy spectra of high-frequency electron density fluctuations, $k^2 \langle |\mathbf{E}(\mathbf{k})|^2 \rangle$, and low frequency density fluctuations, $\langle |n(\mathbf{k})|^2 \rangle$, from 2D simulations in DuBois et.al. [1994b]. Top panels: Cavitation regime with E_0 equal to 3.4 times the OTSI threshold field and $\Delta\Omega/\omega_{p_e} = 1.8 \times 10^{-3}$ corresponding roughly to the first heater interference maximum. Other parameters: $T_e = T_i, \nu_e(k=0)/\omega_p) = (1/2)(\nu_{ei}/\omega_p) = 2 \times 10^{-5}, \Omega_e/\omega_p = 0.13, m_i/m_e = 6200$ and ion density response determined from the 3-pole model.

Lower panels: High and low frequency electron density spectra in the cascade regime. Parameters the same as above except E_0 is twice the PDI threshold amplitude and $\Delta\Omega/\omega_p = 2.4 \times 10^{-2}$ corresponding to the decay matching height for the Arecibo radar and a heater frequency of about 5 MHz. The dashed curves enclose the modes used to generate the Langmuir filament features shown in Fig. 5. These figures are from DuBois et.al. [1994b].

Fig. 4 Plasma line power spectra, $|\psi(\mathbf{k}, \omega)|^2$, and ion line power spectra, $|n(\mathbf{k}, \omega)|^2$, for the parameters of the lower panels in Fig. 3. From DuBois et.al. [1994b]. ($\psi(\mathbf{k}, \omega)$ is the potential of the Langmuir envelope, $E(\mathbf{B}, \omega) = i\mathbf{k}\psi(\mathbf{k}, \omega)$). θ is the angle (in degrees) between $\mathbf{k}$ and the geomagnetic field. k is measured in units of $2/3\ (m_e/\eta m_i)^{1/2} k_{D_e}$ and n and ψ are in standard dimensionless units times 10^{-6}, DuBois et.al. [1994b]. "FM" indicates the free mode line and the dashed line indicates the heater frequency measured from 0, which is the local plasma frequency. Units of frequency are $(2/3)\ \omega_{p_e}(m_e/\eta m_i)$. Notice that the free mode and caviton components have comparable intensities at smaller k values, whereas, the cavition component tends to dominate at larger k.

Fig. 5 Top panel: $n(x, y)$ constructed from only the modes in the dashed box in the bottom right panel in Fig. 3 for $\langle |n(\mathbf{k})|^2 \rangle$. Contours of negative values of n (density depletions) are plottted showing field aligned filaments. $\mathbf{E}_0$ and $\mathbf{B}_0$ are in the x direction. Bottom panel: $|E(x, y)|^2$ constructed from only the modes lying between the two dashed ellipses in the left and bottom panel in Fig. 3 for $\langle |E(\mathbf{k})|^2 \rangle$. The localized standing wave structures of wavelength π/k_1 (where k_1 is the wavenumber of the primary decay mode) lie mainly in the density throughs of the upper figure.

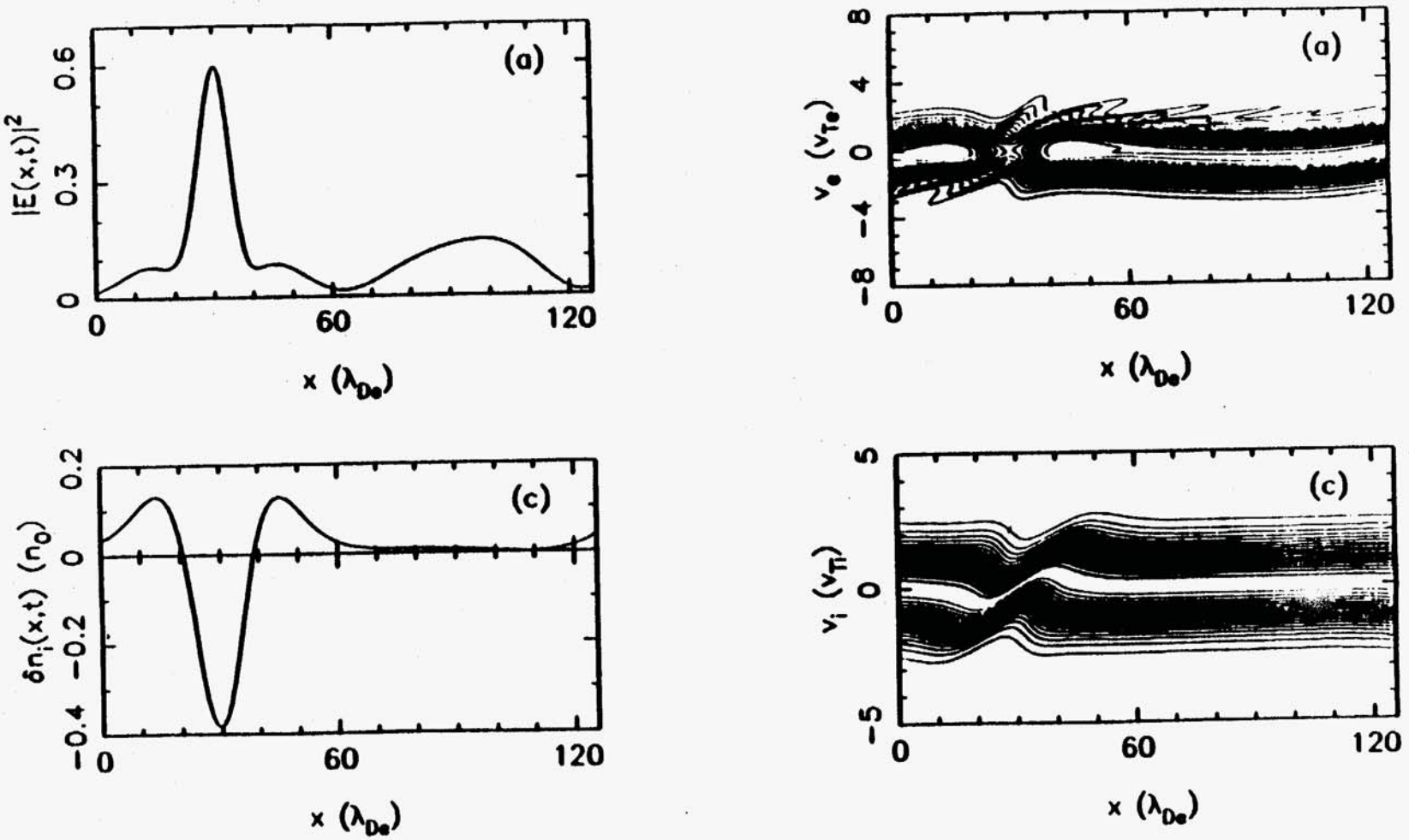
(a)
$|E(x,t)|^2$
0
0.3
0.6
0
60
120
x (λ_{De})
(a)
v_e (v_{Te})
8
4
0
−4
−8
0
60
120
x (λ_{De})
(c)
$\delta n_i(x,t)$ (n_o)
0.2
0
−0.2
−0.4
0
60
120
x (λ_{De})
(c)
v_i (v_{Ti})
5
0
−5
0
60
120
x (λ_{De})

FIGURE 1

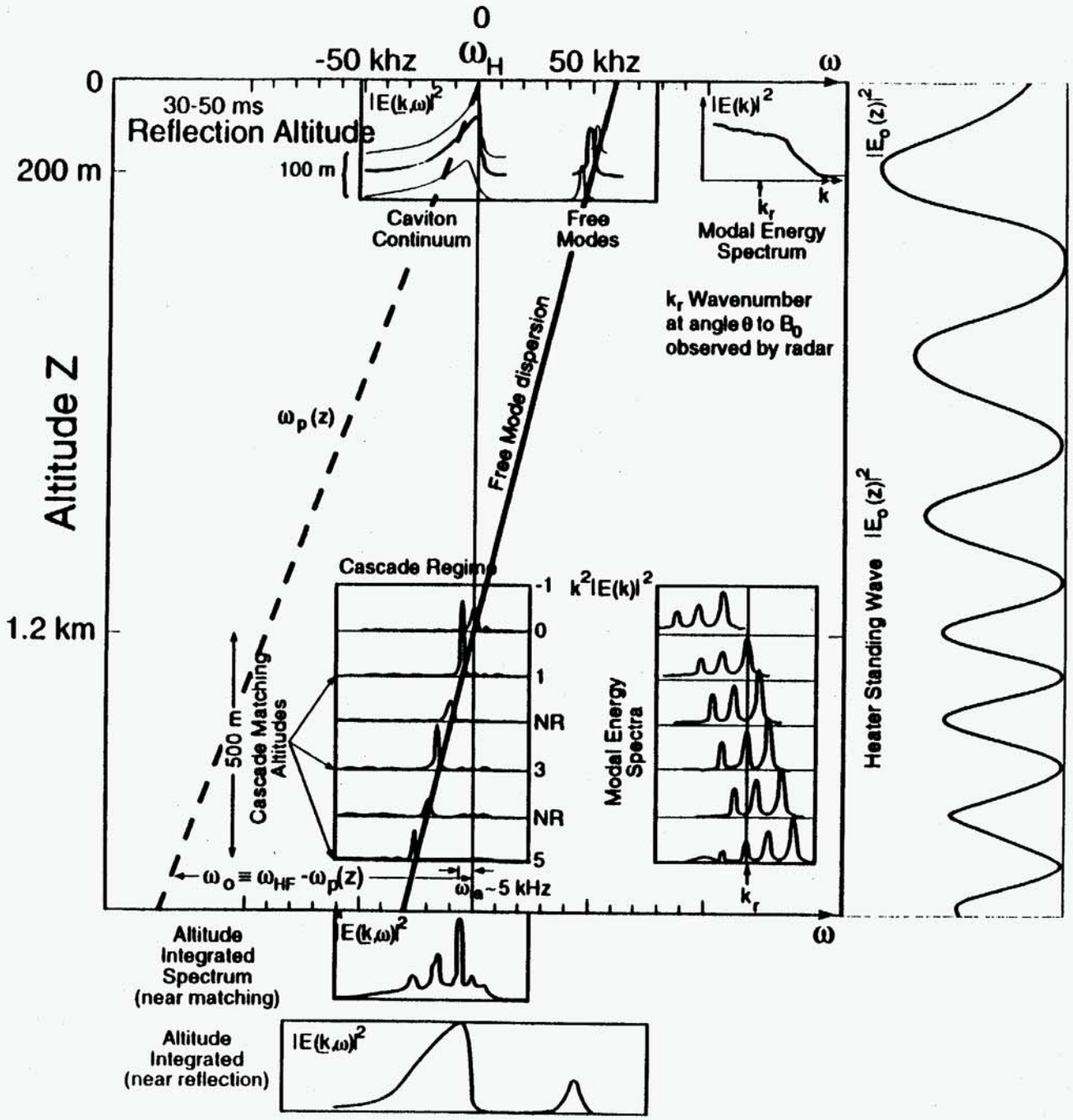
0
-50 khz
ω_H
50 khz
ω
0
30-50 ms
Reflection Altitude
200 m
100 m
$|E(k,\omega)|^2$
Caviton Continuum
Free Modes
$|E(k)|^2$
k_r
k
Modal Energy Spectrum
k_r Wavenumber at angle θ to B_0 observed by radar
$|E_0(z)|^2$
Altitude Z
$\omega_p(z)$
Free Mode dispersion
Cascade Regime
1.2 km
$k^2|E(k)|^2$
-1
0
1
NR
3
NR
5
500 m
Cascade Matching Altitudes
Modal Energy Spectra
$\omega_0 \equiv \omega_{HF} - \omega_p(z)$
ω_e ~5 kHz
k_r
ω
Heater Standing Wave $|E_0(z)|^2$
Altitude Integrated Spectrum (near matching)
$|E(k,\omega)|^2$
Altitude Integrated (near reflection)
$|E(k,\omega)|^2$

FIGURE 2

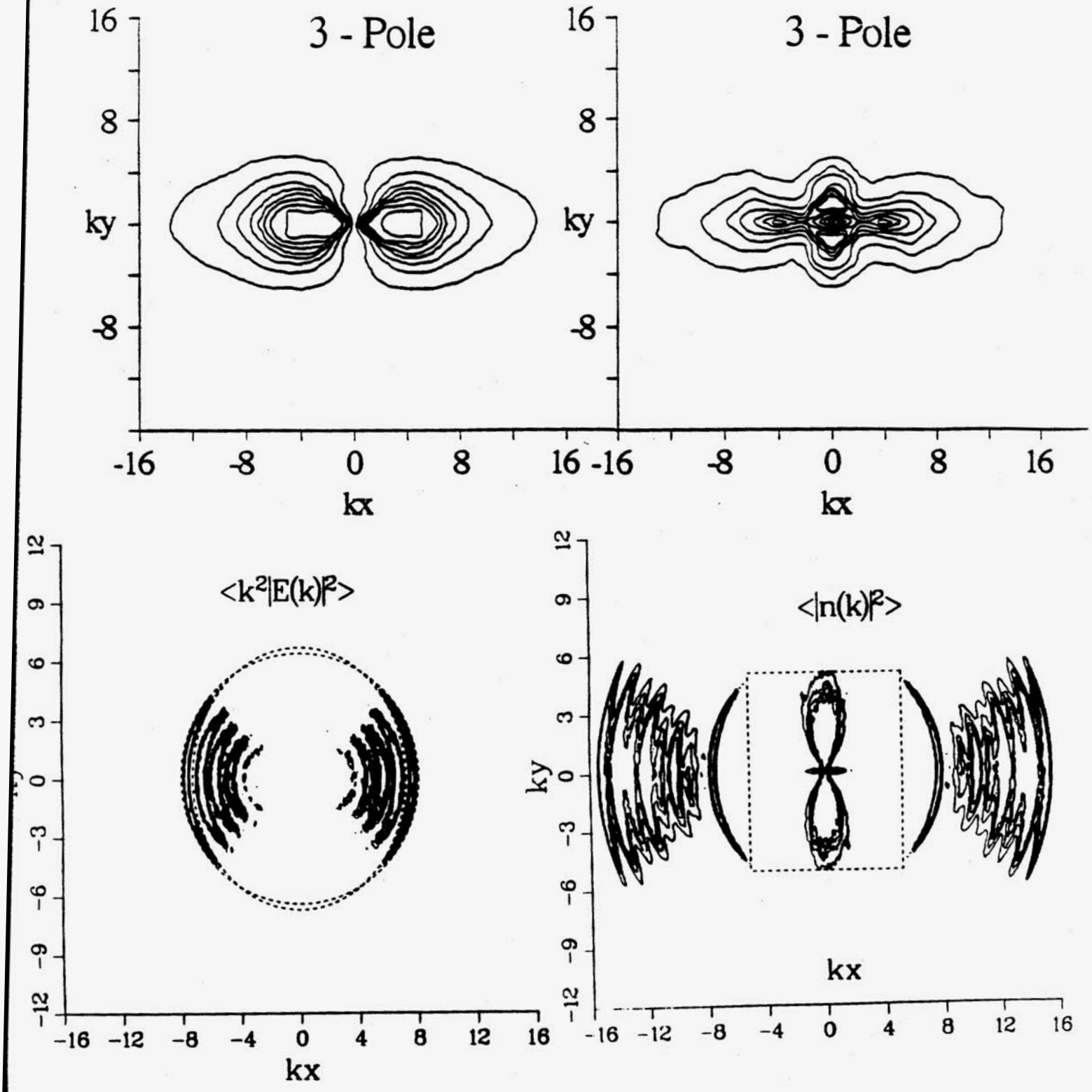

FIGURE 3

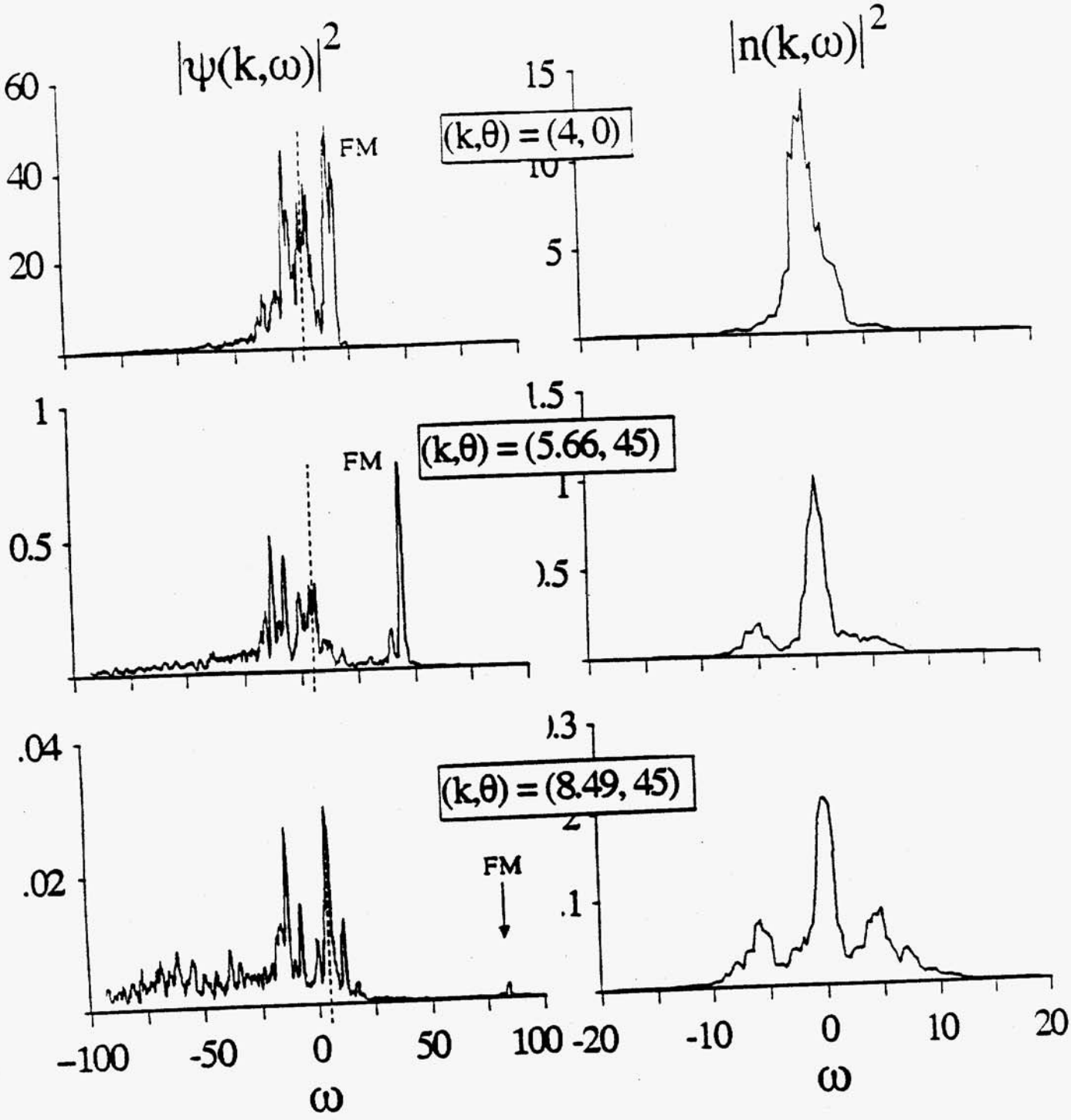
$|\psi(k,\omega)|^2$
$|n(k,\omega)|^2$
(k,θ) = (4, 0)
(k,θ) = (5.66, 45)
(k,θ) = (8.49, 45)
FM
FM
FM
60
40
20
15
10
5
1
0.5
1.5
1
.5
.04
.02
.3
.2
.1
-100
-50
0
50
100
-20
-10
0
10
20
ω
ω

FIGURE 4

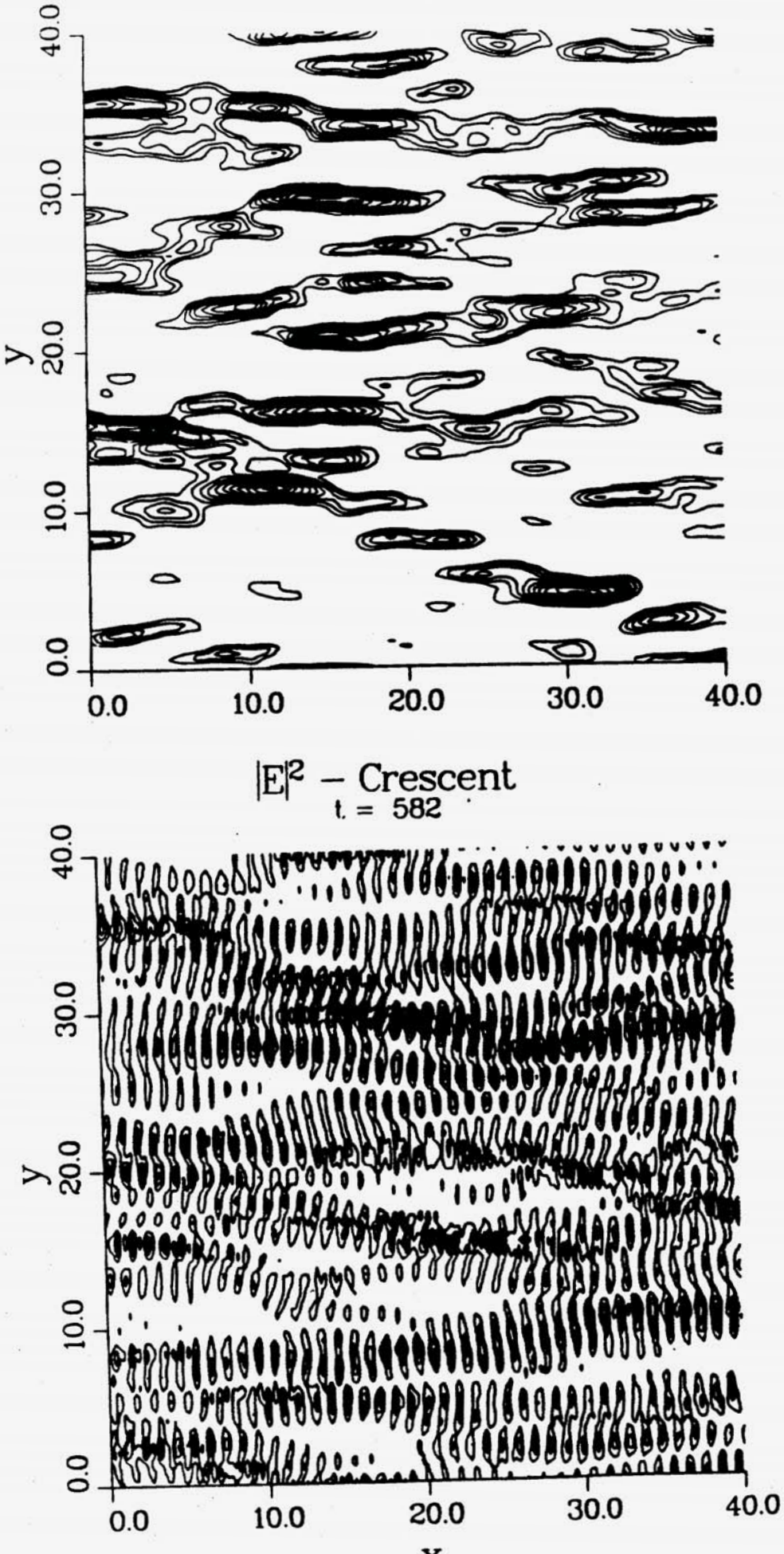
40.0
30.0
20.0
10.0
0.0
y
0.0
10.0
20.0
30.0
40.0
|E|² – Crescent
t. = 582
40.0
30.0
20.0
10.0
0.0
y
0.0
10.0
20.0
30.0
40.0
X

FIGURE 5